1-1-2019

Application of Microgrids in Supporting the Utility Grid

Alireza Majzoobi
University of Denver

Application of Microgrids in Supporting the Utility Grid

Abstract

Distributed renewable energy resources have attracted significant attention in recent years due to the falling cost of the renewable energy technology, extensive federal and state incentives, and the application in improving load-point reliability. This growing proliferation, however, is changing the traditional consumption load curves by adding considerable levels of variability and further challenging the electricity supply-demand balance. In this dissertation, the application of microgrids in effectively capturing the distribution network net load variability, caused primarily by the prosumers, is investigated. Microgrids provide a viable and localized solution to this challenge while removing the need for costly investments by the electric utility on reinforcing the existing electricity infrastructure. A flexibility-oriented microgrid optimal scheduling model is proposed and developed to coordinate the microgrid net load with the aggregated consumers/prosumers net load in the distribution network with a focus on ramping issues and flexibility support of utility grid. The proposed coordination is performed to capture both inter-hour and intra-hour net load variabilities. Furthermore, a microgrid optimal scheduling model is developed to demonstrate microgrid's capability in offering ancillary services to the utility grid. The proposed microgrid optimal scheduling model coordinates the microgrid net load with the aggregated consumers/prosumers net load in its connected distribution feeder to capture both inter-hour and intra-hour net load variations in order to offer different ancillary services to the utility grid. The proposed models are developed through mixed-integer programming. In addition, a robust optimization model is applied to the proposed model in order to consider possible uncertainties in forecasting while supporting the utility grid. The microgrid value of ramping is further determined based on its available reserve using a cost-benefit analysis, which helps the microgrid owners for offering the flexibility support to the utility grid. In addition, a distribution market scheduling model is developed to capture and collect the ramping capability of participating microgrids in the distribution market as to offer it to the upstream network to address emerging ramping issues in the system associated with growing proliferation of variable renewable generation. Moreover, numerical simulations on a test distribution feeder with one microgrid and several consumers and prosumers exhibit the effectiveness of the proposed model.

Document Type
Dissertation

Degree Name
Ph.D.

Department
Electrical Engineering

First Advisor
Amin Khodaei, Ph.D.

Keywords
Distributed generation, Distribution markets, Grid flexibility, Microgrid optimal scheduling, Power distribution, Renewable energy resources

Subject Categories
Computer Engineering | Engineering

APPLICATION OF MICROGRIDS IN SUPPORTING THE UTILITY GRID

A Dissertation

Presented to

the Faculty of the Daniel Felix Ritchie School of Engineering and Computer Science

University of Denver

In Partial Fulfillment

of the Requirements for the Degree

Doctor of Philosophy

---

by

Alireza Majzoobi

June 2019

Advisor: Dr. Amin Khodaei

Author: Alireza Majzoobi
Title: APPLICATION OF MICROGRIDS IN SUPPORTING THE UTILITY GRID
Advisor: Dr. Amin Khodaei
Degree Date: June 2019

Abstract

Distributed renewable energy resources have attracted significant attention in recent years due to the falling cost of the renewable energy technology, extensive federal and state incentives, and the application in improving load-point reliability. This growing proliferation, however, is changing the traditional consumption load curves by adding considerable levels of variability and further challenging the electricity supply-demand balance. In this dissertation, the application of microgrids in effectively capturing the distribution network net load variability, caused primarily by the prosumers, is investigated. Microgrids provide a viable and localized solution to this challenge while removing the need for costly investments by the electric utility on reinforcing the existing electricity infrastructure. A flexibility-oriented microgrid optimal scheduling model is proposed and developed to coordinate the microgrid net load with the aggregated consumers/prosumers net load in the distribution network with a focus on ramping issues and flexibility support of utility grid. The proposed coordination is performed to capture both inter-hour and intra-hour net load variabilities. Furthermore, a microgrid optimal scheduling model is developed to demonstrate microgrid's capability in offering ancillary services to the utility grid. The proposed microgrid optimal scheduling model coordinates the microgrid net load with the aggregated consumers/prosumers net load in its connected distribution feeder to capture both inter-hour and intra-hour net load variations in order to offer different ancillary services to the utility grid. The proposed models are developed

through mixed-integer programming. In addition, a robust optimization model is applied to the proposed model in order to consider possible uncertainties in forecasting while supporting the utility grid. The microgrid value of ramping is further determined based on its available reserve using a cost-benefit analysis, which helps the microgrid owners for offering the flexibility support to the utility grid. In addition, a distribution market scheduling model is developed to capture and collect the ramping capability of participating microgrids in the distribution market as to offer it to the upstream network to address emerging ramping issues in the system associated with growing proliferation of variable renewable generation. Moreover, numerical simulations on a test distribution feeder with one microgrid and several consumers and prosumers exhibit the effectiveness of the proposed model.

Acknowledgment

First and foremost, I would like to express my sincere gratitude to my advisor, Dr. Amin Khodaei, for his valuable academic guidance, encouragement and continuous support throughout my research and study. I was privileged to be advised by him during my doctoral studies and I am forever grateful for his endless supports.

Besides my advisor, I would like to cordially thank my committee members, Dr. Andrew Goetz, Dr. David Gao, and Dr. Mohammad Matin for their time, feedbacks and support. My thanks also go to JB Holston, Dean of Ritchie School of Engineering and Computer Science, for his supports.

I deeply thank my parents and my sister for their endless love, unconditional support and encouragement. They live in my home country, Iran, and I have not seem them for several years. Words cannot express how grateful I am to them for all of the sacrifices, supports and encouraging me with their best wishes.

A special thanks to my wonderful wife, Sara, and my sweet daughter, Hilla. I know I have dedicated all the times which belong to you to my research and I cannot thank you enough for your patience and sacrifices throughout these recent years. Thanks for your moral support and encouragement.

Finally, I would also like to thank all my dear colleagues and friends at University of Denver and all friends in Denver.

Table of Contents

List of Figures

List of Tables

Nomenclature

Abbreviations

DER	Distributed Energy Resource
DES	Distributed Energy Storage
DG	Distributed Generation
DMO	Distribution Market Operator
DSO	Distribution System Operator
ISO	Independent System Operator
MIP	Mixed Integer Programming
NERC	North American Electric Reliability Corporation
VOLL	Value of Lost Load

Indices

b	Index for buses
c	Superscript for distribution network consumers and prosumers
ch	Superscript for DES charging mode
dch	Superscript for DES discharging mode
d	Index for loads
f	Superscript for fixed loads
g	Index for segments of the load/ramping bids.
h	Index for time periods (day)
i	Index for DERs
j	Index for consumers/prosumers at the distribution network
k	Index for intra-hour time periods
m	Index for microgrids
r	Superscript for responsive loads
s	Index for scenarios
t	Index for inter-hour time periods
u	Superscript for the utility grid

Sets

D	Set of dual variables
F	Set of flexibility constraints
G	Set of all dispatchable units
N	Set of consumers/prosumers
O	Set of operation constraints
P	Set of primal variables
S	Set of DESs
U	Set of uncertain parameters
W	Set of non-dispatchable units

Parameters

c	Marginal cost of dispatchable units
d	Load demand
D	The demand awarded from the ISO to the DMO
D^f	Total fixed load of all microgrids in the distribution network
DX^{max}	Maximum segment quantity
DR	Ramp down rate
DT	Minimum down time
E	Load total required energy
$F(.)$	Generation cost
N_g	Number of segments in demand bid
M	Large positive number
MC	Minimum charging time
MD	Minimum discharging time
MU	Minimum operating time
UR	Ramp up rate
UT	Minimum up time

w Binary islanding indicator (1 if grid-connected, 0 if islanded)

α, β Specified start and end times of adjustable loads

ρ Market price

η Energy efficiency of DESs

λ Value of lost load (VOLL)

ψ Probability of islanding scenarios

τ Time period

μ Microgrid value of ramping

ε Small positive number

$\mathit{\Delta}$ Desired ramping of the utility grid

Δ_1 Intra-hour flexibility limit

Δ_2 Inter-hour flexibility limit

$\Delta_1^{low}/\Delta_1^{up}$ Microgrid time-dependent intra-hour lower/upper flexibility limit

$\Delta_2^{low}/\Delta_2^{up}$ Microgrid time-dependent inter-hour lower/upper flexibility limit

Variables

C Energy storage available (stored) energy

D Load demand

DX The amount of load awarded to each bid segment

I Commitment state of dispatchable units (1 when committed, 0 otherwise)

LS Load curtailment

P DER output power

PD^M Assigned demand to microgrids by the DMO

P^M Utility grid power exchange with the microgrid

RR Ramping rate of dispatchable units

RR^{Sel} Selected ramping rate of each microgrid

RR^{Total} Total ramping capability of all microgrids

SD Shut down cost

SL_1, SL_2 Slack variables

SU Startup cost

T^{ch}	Number of successive charging hours
T^{dch}	Number of successive discharging hours
T^{on}	Number of successive ON hours
T^{off}	Number of successive OFF hours
u	Energy storage discharging state (1 when discharging, 0 otherwise)
v	Energy storage charging state (1 when charging, 0 otherwise)
z	Adjustable load state (1 when operating, 0 otherwise)
δ	Binary variable representing the selected bid segment

1. Chapter One: Introduction

The evolution of renewable energy over the past few decades has surpassed all expectations, due to significant advantages that they offer, such as reduced operation cost, air pollution reduction, and benefiting from the ubiquitous source of energy. Total worldwide renewable power capacity (excluding large hydro) has been dramatically increased from 85 GW in 2004 to 921 GW by the end of 2016 and 1,081 GW by end of 2018 [1]–[3]. However, despite the benefits, renewable energy resources challenge the traditional grid management practices, thus their likely impacts on the grid should be also considered. The growing trend of renewable generation installations in the United States, driven primarily by current renewable portfolio standards in 27 states, efficiency incentives and net metering in 43 states, and the falling cost of renewable generation technologies [4], [5], challenges traditional practices in balancing electricity supply and demand and calls for innovative methods to reduce impacts on grid stability and reliability.

For instance, rapid growth of solar energy as one of the most favorable distributed generation technologies adopted by end-use customers, has changed the typical daily demand curves. A typical daily demand curve rises in the morning and peaks in the afternoon, (especially in the summer as air conditioners are extensively used) and it hits a second highest peak in the early evening. The solar energy resources, however, usually generate the highest amount of power at the noontime and decrease toward sunset, hence they offer the capability of supplying the around-noon power demand but have a marginal effect on early evening peaks. Therefore, rapid growth of solar energy has led to changing traditional afternoon peaks to afternoon valleys which are followed by a steep and problematic peak in early evening hours [6], [7]. Fig. 1.1 shows daily net load (i.e., the consumer load minus local generation) variations in California, the so-called "duck curve", as an example of this challenge [7]. In 2013, the California Independent System Operator (CAISO) published this chart depicting the predicted demand curve and potential for "over-generation" occurring at increased penetration of solar energy. The introduced demand curve by CAISO, depicts the potential of solar energy to provide more energy than what can be used by the system in the early afternoon and a severe ramp up in the early evening. This over generation and severe ramp-up in the revised demand curve would be a pressing issue for the utility companies as they may require additional fast response generation units to respond quickly to this change. This ramping effect becomes more severe as the solar energy penetration increases in the power system.

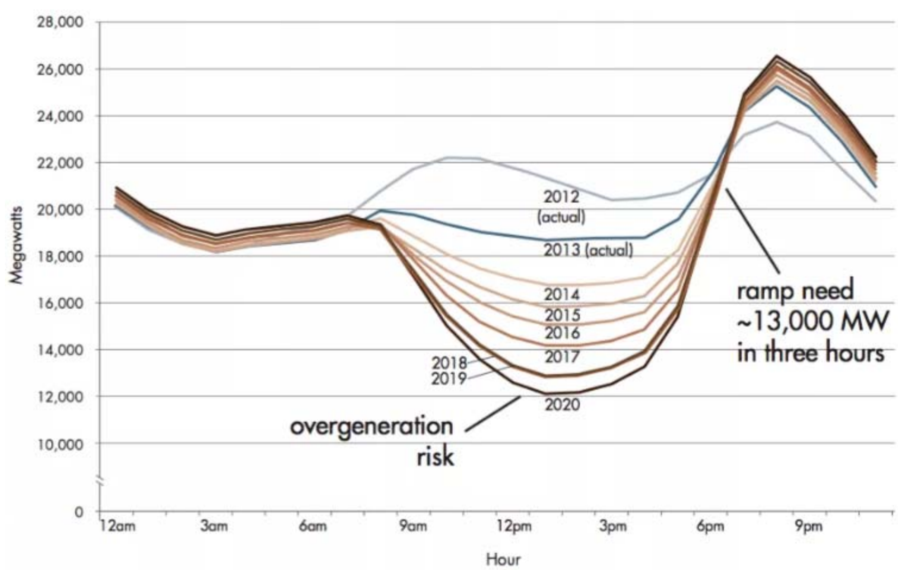

Fig. 1.1 The current and future estimates of over-generation and ramping effect in California [7].

As the figure shows the belly of the duck, where solar generation is at a maximum, grows with deployment of solar energy between 2012 and 2020. As renewable generation increases, to reach the 33% renewable target by 2020 and specifically supply 20% of the U.S. power consumption by solar energy until 2030, the power grid would require increased levels of fast ramping units to address abrupt changes (as much as 13 GW in three hours) in the net load, caused by concurrent fall in renewable generation and increase in demand.

Maintaining the supply-load balance is of utmost importance to system operators which is now further challenged with this significant increase in variable renewable generation [8]. Although considerable efforts have been devoted to predicting electricity demand [9]–[11] and accurate forecasting of renewable power generation has been a major area of research in power systems in the last decade [12]–[18], it is still impossible to predict electricity demand with complete accuracy, i.e. without any forecast errors [19]. The seconds to minutes timescale load and generation variation needs relatively rapid response in order to maintain a balanced system which is usually addressed by Automatic Generation Control via frequency regulation [19], [20]. In timescales of minutes to hours, slightly slow but large magnitude variations in the net load are captured via load following. While in hours to days timescales, forecasted load (which includes variabilities and ramping) should be met via unit commitment [20].

Renewable energy deployment increases the required ramping and load following services in power systems where higher penetrations would make this challenge more difficult to address [21]. Considerable amount of research is carried out in recent years to assess the effect of renewable energy penetration on the flexibility requirements of power systems, as well as mitigation of associated generation variability and uncertainty via managing the system flexibility [22]–[26]. In [24], the power system day-ahead flexibility requirements are determined via net load volatility characterization. The study in [27] proposes a method for quantifying power system's flexibility over different time horizons, while the study in [28] defines the flexibility potential dynamics of the power system and its individual resources, with introducing the concept of the flexibility envelope. To maintain system supply-load balance, system operators traditionally rely on load-following schemes enabled by fast hydroelectric generators or thermal units, and not the baseload generation units, such as nuclear or coal-fired, that have technical restrictions for fast ramping [29]. It is commonly enabled by quantifying the spinning reserve requirements by grid operators [30]. However, larger spinning reserve amounts increase the operation cost and decrease the power system efficiency. The renewable generation integration problem can be investigated under two contexts of large-scale (which attempts to manage the generation of wind and solar farms) [27], [31]–[33], and small-scale (which deals with renewable generation in the distribution level). Small-scale coordination approaches mainly focus on various methods of demand side management, such as demand response [34]–[41], energy storage [20], [29], [42]–[47] and aggregated electric vehicles [48], [49]. Demand response as a viable solution has received significant attention in recent years. A successful demand response implementation, however, requires investment on the infrastructure, such as intelligent energy systems, advanced metering infrastructure, and smart buildings, and further depends on the customers' willingness to participate in demand response programs [38]–[40]. The net lead variations, due to renewable generation, can also be mitigated by energy storage systems as discussed in [29], [42]–[47], [50]. The studies in [20] and [51] provide a review of different available technologies, advantages and disadvantages of these technologies, and some challenges of energy storage systems for mitigating the variability of renewable generation. Although the application of the energy storage along with renewable resources seems a viable alternative, the large-scale energy storage systems to be used for this purpose are not yet economically viable [52]. The utilization of plug-in electric vehicles is investigated as another alternative for mitigating load variability and ramping [19], [48], [49], [53], [54]. Aggregated electric vehicles deployment offers a large capacity energy storage in the power system. Plug-in electric vehicles further offer great potential as an enabler of demand response, especially for load shifting, via charging at off-peak hours and discharging at peak hours. The results of study in [48] and [53] show that the optimized charging and discharging schedule decreases load peaks and reduces the amount of conventional generation required as backup capacity for supplying net load ramping, compared with uncontrolled charging and discharging. This approach, however, significantly increases the number of charging and discharging of electric vehicles which have a negative impact on the lifetime of their batteries and is not commonly acceptable by vehicle owners. The unpredictability and unavailability of electric vehicles are mentioned as additional barriers in utilizing electric vehicles for net load variation support [49].

Leveraging available flexibility in existing microgrids for addressing renewable generation integration, as proposed in this dissertation will offer a potentially more viable solution to be used in distribution networks, and thus calls for additional studies. The microgrid, as defined by the U.S. Department of Energy, is:

“a group of interconnected loads and distributed energy resources (DER) within clearly defined electrical boundaries that acts as a single controllable entity with respect to the grid and can connect and disconnect from the grid to enable it to operate in both grid-connected or island-mode” [55].

The microgrid, as a novel distribution network architecture with local generation, control, and consumption, offers noticeable benefits to both consumers and utility companies such as enhanced reliability and resilience, reduced environmental impact, power quality improvement, improved energy efficiency by loss reduction, distribution asset management, and network congestion relief. Microgrids can be operated in grid-connected and islanded modes. In the grid-connected mode, which is the default operation mode, the microgrid can import, export, or have zero power exchange with the utility grid to achieve the least-cost supply schedule (i.e., an economic operation). Capability to switch to the islanded mode is the salient feature of the microgrids which isolates the microgrid from faults and/or disturbances in the upstream network to achieve the least load curtailment (i.e., a reliable operation) [56]–[65]. During the grid-connected mode, however, microgrid freely exchanges power with the utility grid which can be in the form of power import or export. If this power exchange is efficiently controlled, by adding proper constraints to the microgrid optimal scheduling framework, the microgrid can be used to capture the generation variability of distributed renewable energy resources in the distribution grid. These flexibility constraints, that enable the microgrid to support the utility grid in terms of flexibility services and providing various ancillary services, are investigated and developed in this study.

Microgrids have been significantly deployed over the past few years and are anticipated to grow even more in the near future [66], [67], in both national and international levels [68]. A global trend can be seen in microgrid deployments, where the microgrids revenue is anticipated to reach $19.9 billion by 2020 [69]. More than 1,500 microgrid projects, with the capacity of 15,600 MW, have been reported until April 2016 and 1,565 MW new microgrid projects have been introduced in 39 countries as new projects [70]. Indeed, future power grids can be pictured as systems of interconnected microgrids [55].

This dissertation mainly focuses on the flexibility advantages of microgrids as a complementary value proposition in grid support. The microgrid capability in managing its power exchange with the utility grid in the grid-connected mode is specifically considered in this research for mitigating the net load ramping in the distribution network and to further ensure that the power seen by the utility has manageable ramps. Microgrids deployment of controllable resources, such as dispatchable generation units, energy storage, and adjustable loads, provides a quick and efficient response for changing the microgrid generation/load, which can be utilized for supporting the grid operation [71]–[74]. This support can be provided for various time resolutions based on utility requirements. There have been several studies that investigate how a microgrid can participate in the upstream network market and offer services to the grid. In [75], an optimal bidding strategy via a microgrid aggregator is proposed to involve all small-scale microgrids into an electricity market via real-time balancing market bidding. In [76], an optimal bidding strategy based on two-stage stochastic linear programming for an electric vehicle aggregator who participates in the day-ahead energy and regulation markets is proposed. Furthermore, it goes on to consider market conditions and the associated uncertainty of the electric vehicle fleet. A two-stage market model for microgrid power exchange with the utility grid, via an aggregator, is proposed in [76] to achieve an efficient market equilibrium. A risk-constrained optimal hourly bidding model for microgrid aggregator is proposed in [77] to consider various uncertainties and maximize the microgrid benefit. The study in [78] proposes an optimal dispatch strategy for the residential loads via artificial neural network for calculating the demand forecast error when the demand changes are known one hour ahead with respect to the day-ahead forecasted values. The study in [79] presents a stochastic bidding strategy for microgrids participating in energy and spinning reserve markets, considering the load and renewable generation uncertainty. In [80], a stochastic look-ahead economic dispatch model for near-real-time power system operation is proposed and its benefits and implement ability for assessing the power system economic risk are further explored. These works primarily rely on a market mechanism to procure microgrids' flexibility and accordingly capture the unbalanced power in the day-ahead market as well as the ramping and variabilities caused by forecast errors or unforeseen real-time events. In this dissertation, however, this problem is studied from a microgrid perspective, i.e., how a microgrid controller can manage local resources to offer required/desired services to the utility grid. Three time resolutions are considered in this study, including hourly (for ramping support), 10-minute based (for load following) and 1-minute based (for frequency regulation). A mixed-integer programming (MIP) model is used to formulate the microgrid optimal scheduling problem subject to prevailing operational and added flexibility constraints. This work is particularly important in networks that a market mechanism cannot be established but grid operators are interested in low-cost and distributed solutions in managing grid flexibility.

The main contributions of this dissertation are listed as follows:

- A flexibility-oriented microgrid optimal scheduling model is developed to optimally manage local microgrid resources while providing ancillary services to the utility grid. This model is achieved by transforming the distribution net load variability limits into constraints on the microgrid net load.
- A coordinated grid-connected and islanded operation is considered in the model development to take into account microgrid's potential islanding while supporting the utility grid in the grid-connected mode.
- A high resolution operation is modeled via consideration of both intra-hour and inter-hour time periods, which is capable of integrating quick variations in renewable generation and offering a variety of ancillary services to the utility grid.
- Three various time resolutions including hourly, 10-minute based, and minute-based are considered respectively for ramping support, load following, and frequency regulation as ancillary services to the utility grid.
- Microgrid value of ramping is calculated which could be a decisive factor for microgrid operator to whether participate in supporting distribution network flexibility or not.
- A distribution market scheduling model is developed to capture and collect the ramping capability of participating microgrids in the distribution market as to offer it to the upstream network.

The rest of the dissertation is organized as follows. A flexibility-oriented microgrid optimal scheduling model is proposed and developed in Chapter Two to support distribution grid flexibility through coordinating the microgrid net load with the aggregated consumers/prosumers net load in the distribution network. In Chapter Three, a microgrid optimal scheduling model is developed to demonstrate microgrid's capability in offering different ancillary services to the utility grid. In chapter Four, the possible uncertainties in forecasting of load, renewable generation, and market price are further considered in the proposed model via robust optimization method. The microgrid value of ramping is determined in Chapter Five, based on its available reserve using a cost-benefit analysis. In Chapter Six, a distribution market scheduling model is proposed to collect the ramping capability of participating microgrids in the distribution market to offer it to the upstream network. All the proposed models are tested on a test microgrid to show their merits and effectiveness. Finally, the conclusion and the future directions are provided in Chapter Seven.

2. Chapter Two: Supporting Distribution Grid Flexibility

2.1 Distribution Grid Flexibility Support Model Outline

A model for leveraging available flexibility of microgrids to support distribution grid flexibility is proposed in this section. Consider a distribution feeder consisting of a set N = {1, 2, …, N} customers (both consumers and prosumers) and one microgrid. The net load of each customer $j \in$ N and the microgrid are respectively denoted by P_{jtk}^{c} and P_{tk}^{M}, where t is the inter-hour time index and k is the intra-hour time index as demonstrated in Fig. 2.1.

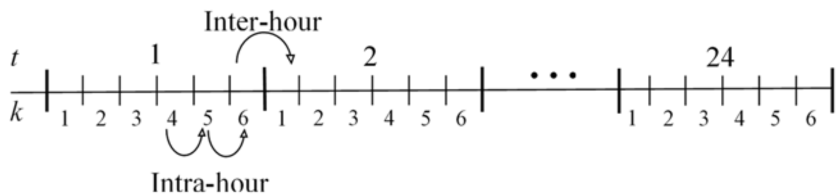

Fig. 2.1. The schematic diagram of inter-hour and intra-hour time intervals.

To fully supply the total net load in this feeder, a power of P_{tk}^{u} needs to be provided by the utility grid where:

$$P_{tks}^{u} = P_{tks}^{M} + \sum_{j \in N} P_{jtks}^{c} \qquad \forall t, \forall k, \forall s. \tag{2.1}$$

To address the net load variability seen by the grid operator, the intra-hour variability (2.2) and inter-hour variability (2.3) in the utility grid power will need to be constrained:

$$\left|P^u_{tks} - P^u_{t(k-1)s}\right| \le \Delta_1 \qquad \forall t, \forall s,\ k \ne 1, \tag{2.2}$$

$$\left|P^u_{t1s} - P^u_{(t-1)Ks}\right| \le \Delta_2 \qquad \forall t, \forall s. \tag{2.3}$$

These limits are selected by the grid operator based on the day-ahead net load forecasts and desired grid flexibility during each time interval. There are various methods to determine the grid flexibility [21], [24], [27]. If this calculated flexibility is less than the required grid flexibility, which is obtained based on net load forecasts, the grid operator can utilize distributed resources, such as microgrids, to compensate the shortage in grid flexibility. Therefore, intra- and inter-hour limits will be obtained by comparing the available and required grid flexibility. Considering the importance of grid flexibility limits on the microgrid operation, a system-level study needs to be performed by the utility company. This topic will be investigated in a follow up research. The grid operator furthermore can calculate these limits using a cost-benefit analysis, i.e., to upgrade the current infrastructure to address increasing flexibility requirements or to procure the flexibility of existing microgrids and in turn pay for their service. This topic, however, requires further analysis and modeling which will be carried out in follow up research.

Fig. 2.2 shows the schematic diagram of a feeder consisting of a microgrid along with other connected loads. The microgrid can be scheduled based on price considerations, i.e., local resources are scheduled in a way that the microgrid operation cost is minimized during the grid-connected mode (Fig. 2.2-top). The only factor impacting the microgrid scheduling results from the utility grid side is the real-time electricity price (hence the term price-based scheduling). The price-based scheduling can potentially exacerbate the consumption variability. On the other hand, microgrid resources can be scheduled in coordination with other loads in the same distribution feeder, and thus support the utility grid in mitigating potential variabilities and ensuring supply-load balance (Fig. 2.2-bottom). Although the objective is still to minimize the operation cost during the grid-connected mode, this scheduling is primarily based on the grid flexibility requirements (hence the term flexibility-oriented scheduling)[81].

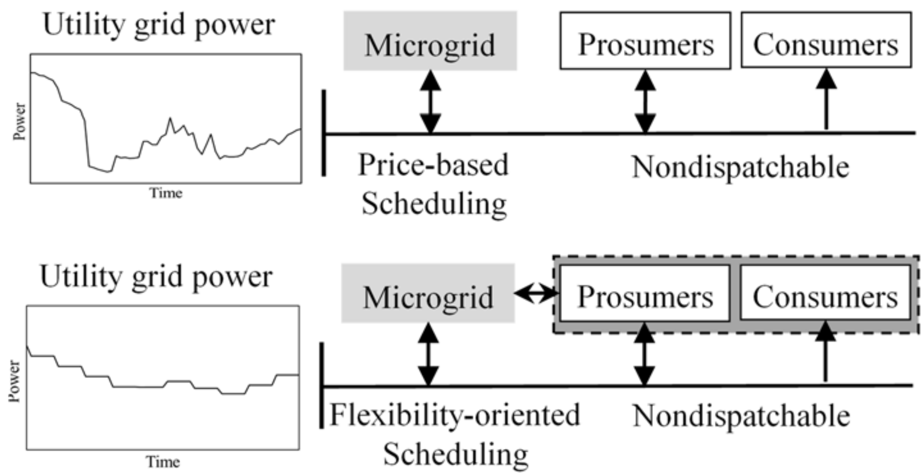

Fig. 2.2. Impact of the microgrid in increasing the distribution net load variabilities (top) or capturing the variabilities (bottom).

2.2 Flexibility-Oriented Microgrid Scheduling Problem Formulation

The microgrid optimal scheduling problem aims at determining the least-cost schedule of available resources (DERs and loads) while considering prevailing operational constraints, i.e.,

$$\min \sum_t \sum_k \tau [\sum_{i\in G} F_i(P_{itk0}) + \rho_t^M P_{tk0}^M] + \sum_t \sum_k \sum_s \tau\, \psi_s\, \lambda\, LS_{tks} \tag{2.4}$$

Subject to

$$\sum_i P_{itks} + P_{tks}^M + LS_{tks} = \sum_d D_{dtks} \qquad \forall t, \forall k, \forall s, \tag{2.5}$$

$$-P^{M,\max} w_{tks} \le P_{tks}^M \le P^{M,\max} w_{tks} \qquad \forall t, \forall k, \forall s, \tag{2.6}$$

$$\{P_{itks}, D_{dtks}\} \in \mathrm{O}_s \qquad \forall i, \forall t, \forall k, \forall s, \qquad (2.7)$$

$$P_{tks}^{M} \in \mathrm{F}_s \qquad \forall t, \forall k, \forall s. \qquad (2.8)$$

The objective (2.4) minimizes the microgrid daily operation cost, which includes the local generation cost, cost of energy transfer with the utility grid, and the outage cost. The outage cost (also known as the cost of unserved energy) is defined as the load curtailment times the value of lost load (VOLL). The VOLL represents the customers' willingness to pay for reliable electricity service and to avoid power outages, which can also be perceived as the energy price for compensating curtailed loads. The VOLL depends on the type of customers, time and duration of outage, time of advanced notification of outage, and other specific traits of an outage. The VOLL is generally considered between \$0/MWh and \$17,976/MWh for residential customers, while for commercial and industrial customers is estimated between \$3,000/MWh and \$53,907/MWh [82]. The load balance equation (2.5) ensures that the sum of the injected/withdrawn power from the utility grid and local DERs (i.e., dispatchable units, nondispatchable units, and the distributed energy storage) would match the microgrid load. The load curtailment variable is used to ensure a feasible solution in the islanded operation if adequate generation is not available. The power of energy storage can be negative (charging), positive (discharging) or zero (idle). Since the power can be exchanged between the utility grid and the microgrid, P_{tks}^{M} can be positive (power import), negative (power export) or zero. The power transfer with the utility grid is limited by (2.6). The binary islanding parameter (which is 1 when grid-connected and 0 when islanded) ensures that the microgrid interacts with the utility grid only during the grid-connected operation. Microgrid DERs, loads, and the main grid power transfer are further subject to operation and flexibility constraints, respectively represented by sets O_s and F_s in (2.7)-(2.8).

2.2.1 Operation Constraints (O_s)

The microgrid components to be modeled in the optimal scheduling problem include DERs (i.e., generation units and energy storage) and loads. Microgrid loads are categorized into two types of fixed (which cannot be altered and must be satisfied under normal operation conditions) and adjustable (which are responsive to price variations and/or controlling signals). Generation units in a microgrid are either dispatchable (i.e., units which can be controlled by the microgrid controller) or nondispatchable (i.e., wind and solar units which cannot be controlled by the microgrid controller since the input source is uncontrollable). The primary applications of the energy storage are to coordinate with generation units for guaranteeing the microgrid generation adequacy, energy shifting, and islanding support. From these microgrid components, only dispatchable DGs, energy storage, and adjustable loads can provide flexibility benefits for the microgrid due to their controllability. Microgrid component constraints are formulated as follows:

$$P_i^{\min} I_{it} \le P_{itks} \le P_i^{\max} I_{it} \qquad \forall i \in G, \forall t, \forall k, \forall s, \tag{2.9}$$

$$P_{itks} - P_{it(k-1)s} \le UR_i \qquad \forall i \in G, \forall t, \forall s, k \ne 1, \tag{2.10}$$

$$P_{it1s} - P_{i(t-1)Ks} \le UR_i \qquad \forall i \in G, \forall t, \forall k, \forall s, \tag{2.11}$$

$$P_{it(k-1)s} - P_{itks} \le DR_i \qquad \forall i \in G, \forall t, \forall s, k \ne 1, \tag{2.12}$$

$$P_{i(t-1)Ks} - P_{it1s} \le DR_i \qquad \forall i \in G, \forall t, \forall k, \forall s, \tag{2.13}$$

$$T_i^{on} \ge UT_i (I_{it} - I_{i(t-1)}) \qquad \forall i \in G, \forall t, \tag{2.14}$$

$$T_i^{off} \ge DT_i (I_{i(t-1)} - I_{it}) \qquad \forall i \in G, \forall t, \tag{2.15}$$

$$P_{itks} \le P_{itk}^{dch,\max} u_{it} - P_{itk}^{ch,\min} v_{it} \qquad \forall i \in S, \forall t, \forall k, \forall s, \tag{2.16}$$

$$P_{itks} \ge P_{itk}^{dch,\min} u_{it} - P_{itk}^{ch,\max} v_{it} \qquad \forall i \in S, \forall t, \forall k, \forall s, \tag{2.17}$$

$$u_{it} + v_{it} \le 1 \qquad \forall i \in S, \forall t, \tag{2.18}$$

$$C_{itks} = C_{it(k-1)s} - (P_{itks} u_{it} \tau / \eta_i) - P_{itks} v_{it} \tau \qquad \forall i \in S, \forall t, \forall s, k \ne 1, \tag{2.19}$$

$$C_{it1s} = C_{i(t-1)Ks} - (P_{it1s} u_{it} \tau / \eta_i) - P_{it1s} v_{it} \tau \qquad \forall i \in S, \forall t, \forall s, \tag{2.20}$$

$$C_i^{\min} \le C_{itks} \le C_i^{\max} \qquad \forall i \in S, \forall t, \forall k, \forall s, \tag{2.21}$$

$$T_{it}^{ch} \ge MC_i (u_{it} - u_{i(t-1)}) \qquad \forall i \in S, \forall t, \tag{2.22}$$

$$T_{it}^{dch} \ge MD_i (v_{it} - v_{i(t-1)}) \qquad \forall i \in S, \forall t, \tag{2.23}$$

$$D_d^{\min} z_{dtk} \le D_{dtks} \le D_d^{\max} z_{dtk} \qquad \forall d \in D, \forall t, \forall k, \forall s, \tag{2.24}$$

$$T_d^{on} \ge MU_d (z_{dt} - z_{d(t-1)}) \qquad \forall d \in D, \forall t, \tag{2.25}$$

$$\sum_{[\alpha,\beta]} D_{dtks} = E_d \qquad \forall d \in D,\ \forall s. \tag{2.26}$$

Constraint (2.9) represents the maximum and minimum generation capacity of dispatchable units. The binary variable I represents the unit commitment state which would be one when the unit is committed and zero otherwise. Dispatchable generation units are also subject to ramp up and ramp down constraints which are defined by (2.10)-(2.13). Equations (2.10) and (2.12) represent the ramping constraints for intra-hour intervals, while (2.11) and (2.13) represent the ramping constraint for inter-hour intervals. The minimum up and down time limits are imposed by (2.14) and (2.15) respectively. The minimum and maximum limits of the energy storage charging and discharging, based on the operation mode, are defined by (2.16) and (2.17), respectively. While charging, the binary charging state v is one and the binary discharging state u is zero; while in the discharging mode, the binary charging state v is zero and the binary discharging state u is one. The energy storage charging power is a negative value which is compatible with the negative amount for limitations of constraints (2.16) and (2.17) for the charging mode. Only one of the charging or discharging modes at every time period is possible, which is ensured by (2.18). The energy storage stored energy is calculated based on the available stored energy and the amount of charged/discharged power, which is represented in (2.19) and (2.20) for intra-hour and inter-hour intervals, respectively. The time period of charging and discharging is considered to be $\tau=(1/K)h$, where K is the number of intra-hour periods and h represents a time period of one hour. The amount of stored energy in energy storage is restricted with its capacity (2.21). The minimum charging and discharging times are represented in (2.22) and (2.23), respectively. Adjustable loads are subject to minimum and maximum rated powers (2.24), where binary operating state z is 1 when load is consuming power and 0 otherwise. The minimum operating time (2.25), and the required energy to complete an operating cycle (2.26) are further considered for adjustable loads. It is worth mentioning that $t=0$, which would appear in (2.3), (2.14), (2.15), (2.22), and (2.23), represents the last hour of the previous scheduling horizon, here $t=24$.

2.2.2 Flexibility Constraints (F_s)

Flexibility constraints represent additional limits on the microgrid power exchange with the utility grid. These constraints are defined in a way that the microgrid net load is matched with the aggregated net load of connected prosumers/consumers, so as to capture likely variations. To obtain the flexibility constraints, the value of P^u_{tks}, i.e., $P^u_{tks} = P^M_{tks} + \sum_{j\in N} P^c_{jtks}$, is substituted in (2.2) and (2.3). By proper rearrangements, the inter-hour and intra-hour flexibility constraints will be accordingly obtained as in (2.27) and (2.28):

$$-\Delta_1-(\sum_j P^c_{jtk}-\sum_j P^c_{jt(k-1)})\le P^M_{tks}-P^M_{t(k-1)s}\le\Delta_1-(\sum_j P^c_{jtk}-\sum_j P^c_{jt(k-1)})\qquad\forall t,\forall s,k\ne 1,\tag{2.27}$$

$$-\Delta_2-(\sum_j P^c_{jt1}-\sum_j P^c_{j(t-1)K})\le P^M_{t1s}-P^M_{(t-1)Ks}\le\Delta_2-(\sum_j P^c_{jt1}-\sum_j P^c_{j(t-1)K})\qquad\forall t,\forall s.\tag{2.28}$$

Accordingly, new time-dependent flexibility limits can be defined as follows

$$\Delta^{low}_{1,tk}=-\Delta_1-(\sum_j P^c_{jtk}-\sum_j P^c_{jt(k-1)})\qquad\forall t,k\ne 1,\tag{2.29}$$

$$\Delta^{up}_{1,tk}=\Delta_1-(\sum_j P^c_{jtk}-\sum_j P^c_{jt(k-1)})\qquad\forall t,\ k\ne 1,\tag{2.30}$$

$$\Delta^{low}_{2,t}=-\Delta_2-(\sum_j P^c_{jt1}-\sum_j P^c_{j(t-1)K})\qquad\forall t,\tag{2.31}$$

$$\Delta^{up}_{2,t}=\Delta_2-(\sum_j P^c_{jt1}-\sum_j P^c_{j(t-1)K})\qquad\forall t.\tag{2.32}$$

These new constraints convert the required flexibility by the grid operator to a limit on the microgrid net load. Although utility grid flexibility limits, i.e., Δ_1 and Δ_2, are constant and determined by the grid operator, the limits on the microgrid net load are highly variable as they comprise the aggregated net load of all N customers in the distribution feeder. Depending on the considered time resolution for forecasts, these limits can change from every 1 minute to every 1 hour in the scheduling horizon. The flexibility limits can be adjusted by the grid operator to achieve the desired net load in the distribution network. For example, a value of zero for Δ_1 would eliminate intra-hour variations.

It is worth mentioning that connected prosumers/consumers are considered as given parameters (forecasted) in the optimization problem. There will be no direct communications between the microgrid and the connected prosumers/consumers, where all communications will be through the grid operator. Therefore, the microgrid only communicates with the grid operator and sends/receives the required data for capturing and mitigating the distribution network net load variabilities.

2.2.3 Islanding Considerations

The islanding is performed to rapidly disconnect the microgrid from a faulty distribution network, safeguard the microgrid components from upstream disturbances, and protect voltage sensitive loads when a quick solution to utility grid voltage problems is not imminent. The time and the duration of such disturbances, however, are not known to microgrids in advance. Islanding is considered in this dissertation via a Θ-k islanding criterion, where $\Theta(=T\times K)$ represents the total number of intra-hour time periods in the scheduling horizon and k represents the number of consecutive intra-hour periods that the microgrid should operate in the islanded mode. To apply this criterion to the proposed model, the binary islanding indicator w is defined and added to the microgrid power exchange constraint (2.6). Several scenarios are defined based on the number of intra-hour time periods (for instance 144 scenarios for 10-minute intra-hour periods), and the value of w in each scenario is obtained based on the Θ-k islanding criterion, i.e., in each scenario w will be 0 for k consecutive intra-hour time periods (imposing an islanded operation) and 1 in other periods (representing the grid-connected operation). Fig. 2.3 shows the first five islanding scenarios, from a total of 144 scenarios, associated with a Θ-4 islanding criterion, which requires that the microgrid be able to operate in the islanded mode for any 4 consecutive intra-hour periods once it is switched to the islanded mode. Further discussions on the Θ-k islanding criterion can be found in [83]. It should be noted that the proposed model is generic and can be applied to any microgrid size without loss of generality.

t	1						2						3						
k	1	2	3	4	5	6	1	2	3	4	5	6	1	2	3	4	5	6	...
Scenario 1	0	0	0	0	1	1	1	1	1	1	1	1	1	1	1	1	1	1	...
Scenario 2	1	0	0	0	0	1	1	1	1	1	1	1	1	1	1	1	1	1	...
Scenario 3	1	1	0	0	0	0	1	1	1	1	1	1	1	1	1	1	1	1	...
Scenario 4	1	1	1	0	0	0	0	1	1	1	1	1	1	1	1	1	1	1	...
Scenario 5	1	1	1	1	0	0	0	0	1	1	1	1	1	1	1	1	1	1	...

Fig. 2.3. First five islanding scenarios associated with a Θ-4 islanding criterion.

2.3 Numerical Simulations

A microgrid with four dispatchable units, two nondispatchable units including wind and solar, one energy storage, and five adjustable loads is used to study the performance of the proposed model. The characteristics of the microgrid DERs and loads, and the hourly market price are tabulated in Tables 2.1 - 2.6 which are borrowed from [83]. The maximum ramping capability of the microgrid, based on the maximum ramping capacity of DERs, is 18 MW/h and the capacity of the line connecting the microgrid to the distribution feeder is assumed to be 10 MW. A VOLL of \$10,000/MWh is considered for the microgrid.

Table 2.1 Characteristics of generating units (D: Dispatchable, ND:Non-Dispatchable)

Unit	Type	Cost Coefficient (\$/MWh)	Min.-Max. Capacity (MW)	Min Up/Down Time (h)	Ramp Up/Down Rate (MW/h)
G1	D	27.7	1-5	3	2.5
G2	D	39.1	1-5	3	2.5
G3	D	61.3	0.8-3	1	3
G4	D	65.6	0.8-3	1	3
G5	ND	0	0-1	-	-
G6	ND	0	0-1.5	-	-

Table 2.2 Characteristics of the energy storage system

Storage	Capacity (MWh)	Min.-Max. Charging/Discharging Power (MW)	Min. Charging/Discharging Time (h)
ESS	10	0.4-2	5

Table 2.3 Characteristics of adjustable loads (S: Shiftable, C: Curtailable)

Load	Type	Min.-Max. Capacity (MW)	Required Energy (MWh)	Initial Star-End time (h)	Min Up Time (h)
L1	S	0-0.4	1.6	11-15	1
L2	S	0-0.4	1.6	15-19	1
L3	S	0.02-0.8	2.4	16-18	1
L4	S	0.02-0.8	2.4	14-22	1
L5	C	1.8-2	47	1-24	24

Table 2.4 Microgrid hourly fixed load

Time	1	2	3	4	5	6
Load	8.73	8.54	8.47	9.03	8.79	8.81
Time	7	8	9	10	11	12
Load	10.12	10.93	11.19	11.78	12.08	12.13
Time	13	14	15	16	17	18
Load	13.92	15.27	15.36	15.69	16.13	16.14
Time	19	20	21	22	23	24
Load	15.56	15.51	14.00	13.03	9.82	9.45

Table 2.5 Generation of non-dispatchable units

Time	1	2	3	4	5	6
G5	0	0	0	0	0.63	0.80
G6	0	0	0	0	0	0
Time	7	8	9	10	11	12
G5	0.62	0.71	0.68	0.35	0.62	0.36
G6	0	0	0	0	0	0.75
Time	13	14	15	16	17	18
G5	0.4	0.37	0	0	0.05	0.04
G6	0.81	1.2	1.23	1.28	1.00	0.78
Time	19	20	21	22	23	24
G5	0	0	0.57	0.60	0	0
G6	0.71	0.92	0	0	0	0

Table 2.6 Hourly market price

Time	1	2	3	4	5	6
Price ($/MWh)	15.03	10.97	13.51	15.36	18.51	21.8
Time	7	8	9	10	11	12
Price ($/MWh)	17.30	22.83	21.84	27.09	37.06	68.95
Time	13	14	15	16	17	18
Price ($/MWh)	65.79	66.57	65.44	79.79	115.45	110.28
Time	19	20	21	22	23	24
Price ($/MWh)	96.05	90.53	77.38	70.95	59.42	56.68

The aggregated consumption profile of consumers/prosumers connected to the system in the same feeder as the microgrid is shown in Fig. 2.4. This figure consists of aggregated values for the distributed solar generation, consumption, and the net load (i.e., difference between the local consumption and generation). The net load should be supplied by the utility grid, and as the figure demonstrates, it includes considerable variabilities due to the local solar generation. The maximum ramping of this net load is 3.3 MW/10-min and the peak net load is 12.9 MW. This net load variability should be satisfied by either fast response units deployed by the utility or locally by the microgrid, where the latter is discussed here. The proposed flexibility-oriented microgrid optimal scheduling model is developed using mixed-integer programming and solved using CPLEX 12.6. It should be noted that the computation time for the studied cases was between 3 and 4 minutes, with an average of 3 min and 22 s.

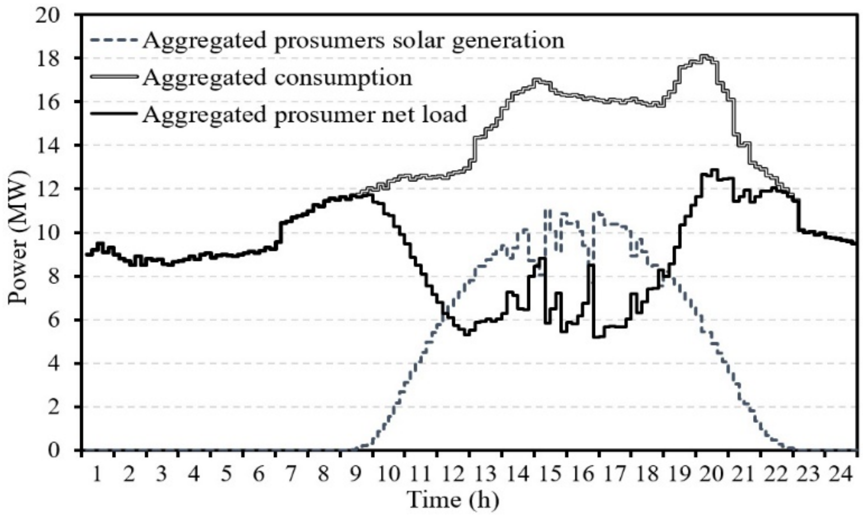

Fig. 2.4. Aggregated prosumers solar generation, consumption, and the net load in the distribution feeder.

Case 1: The grid-connected, price-based optimal scheduling is analyzed for a 24-hour horizon. The price-based scheduling denotes that the microgrid seeks to minimize its operation cost and does not have any commitment to support the utility grid in capturing distribution network net load variabilities. Table 2.7 shows the schedule of dispatchable units and the energy storage for 24 hours of operation in this case. A commitment state of 1 represents that the dispatchable unit is ON while 0 represents that the unit is not committed. The energy storage charging, discharging, and idle states are represented by -1, 1, and 0, respectively. The bold values represent changes in the schedule due to the islanding requirements. Dispatchable unit 1 has the lowest operation cost, so it is committed in all scheduling hours, while other units are committed and dispatched when required based on economic and reliability considerations. It should be noted that the amount of load curtailment during the islanded operation is considered as a measure of microgrid reliability. The energy storage is charged in low price hours and discharged in high price hours, i.e., an energy arbitrage, to maximize the benefits and minimize the operation cost. As the table shows, the islanding criterion leads to the commitment of more units in the grid-connected mode to guarantee a seamless islanding.

Table 2.7 DER Schedule in Case 1

	Hours (1-24)																							
G1	1	1	1	1	1	1	1	1	1	1	1	1	1	1	1	1	1	1	1	1	1	1	1	1
G2	**1**	**1**	**1**	**1**	**1**	**1**	**1**	**1**	**1**	**1**	1	1	1	1	1	1	1	1	1	1	1	1	1	1
G3	**1**	**1**	**1**	**1**	0	0	**1**	**1**	**1**	**1**	**1**	1	1	1	1	1	1	1	1	1	1	1	**1**	**1**
G4	0	0	0	0	0	0	0	0	0	0	0	1	1	1	0	1	1	1	1	1	1	1	0	0
DES	-1	-1	-1	-1	-1	**0**	**0**	0	0	0	0	0	0	0	0	1	1	1	1	1	0	0	0	0

Fig. 2.5 depicts the microgrid net load and the distribution feeder net load (i.e., the microgrid net load plus the aggregated consumer/prosumer net load in Fig. 2.5). As this figure shows, the microgrid imports the power from the utility grid in low price hours and switches over to local generation when the utility grid price is high. This scheduling causes a 21.58 MW peak load for the utility grid between hours 9 and 10 (that is a new morning peak), and also exacerbates the distribution feeder ramping requirement (which is increased to 8.9 MW/10-min between hours 11 and 12 in this case). In addition, the net load variability is significantly increased in this case.

Therefore, the utility grid encounters severe net load ramping and variations, caused by the microgrid to a great extent. This result advocates that the microgrid can potentially have a negative impact on the distribution network net load when scheduled only based on the price data and economic considerations. The microgrid operation cost in this case is $11,748.3.

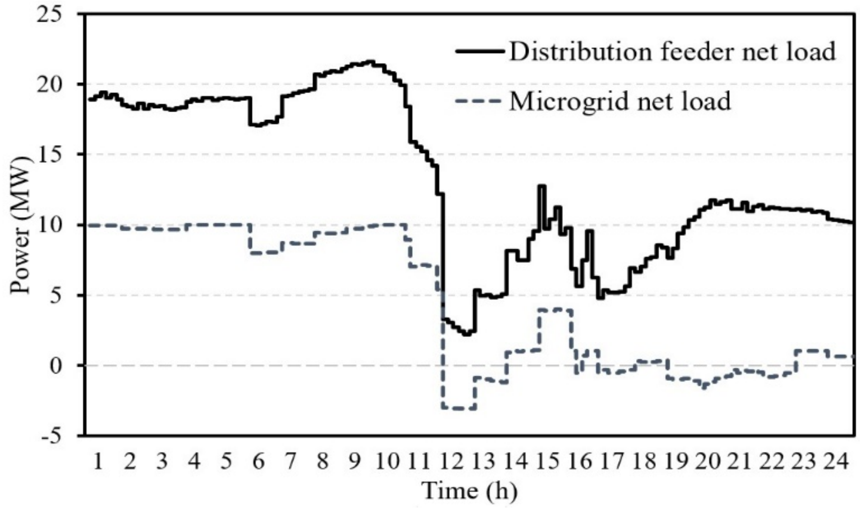

Fig. 2.5. Distribution feeder net load, and microgrid net load for the 24-hour horizon in Case 1.

Case 2: In this case, the flexibility-oriented microgrid optimal scheduling is carried out, rather than the price-based scheduling, to support the utility grid in addressing net load variations. A Θ-1 islanding criterion with 10-min intra-hour periods is considered. This islanding criterion ensures that the microgrid is capable of switching to the islanded mode to reliably supply local loads (for any 10-min islanding during the scheduling horizon), while supporting the utility grid by providing required flexibility during the grid-connected operation. The flexibility limits of 0.5 MW/10-min are considered for inter-hour and intra-hour ramping. The intra-hour and inter-hour ramping constraints are accordingly developed, as proposed in (2.27)-(2.32) and added to the developed model. Table 2.8 shows the schedule of dispatchable units and the energy storage for the scheduling horizon. The bold values represent changes in the schedule, while the highlighted cells represent changes in the dispatched power compared to Case 1. This table shows that the commitment of unit 4 and the energy storage, as well as the dispatched power of all DERs, are changed compared to Case 1 to satisfy the flexibility constraints. These changes in the schedules increase the microgrid operation cost to $12,077. The difference between this cost and the microgrid operation cost in Case 1 should be paid to the microgrid, as a minimum, to incentivize the microgrid for providing flexibility and supporting the utility grid. Fig. 2.6 shows the distribution feeder net load and the microgrid net load in this case.

Table 2.8 DER Schedule in Case 2

	Hours (1-24)																							
G1	1	1	1	1	1	1	1	1	1	1	1	1	1	1	1	1	1	1	1	1	1	1	1	1
G2	1	1	1	1	1	1	1	1	1	1	1	1	1	1	1	1	1	1	1	1	1	1	1	1
G3	1	1	1	1	0	0	1	1	1	1	1	1	1	1	1	1	1	1	1	1	1	1	1	1
G4	0	0	0	0	0	0	0	0	0	**1**	**1**	**0**	1	1	1	1	1	1	1	1	1	1	0	0
DES	**0**	-1	-1	-1	-1	**-1**	**-1**	0	0	0	0	0	0	**1**	**1**	1	1	1	1	1	**1**	0	0	0

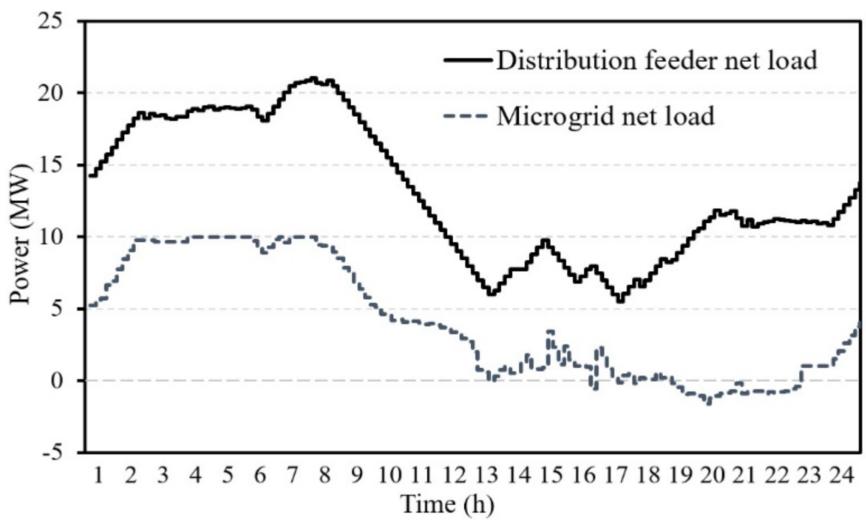

Fig. 2.6. Distribution feeder net load, and microgrid net load for 0.5 MW/10-min inter-hour and intra-hour utility ramping in Case 2.

Comparison of Figs 2.5 and 2.6 shows the positive impact of the microgrid in changing the distribution network net load in a way that is desirable for the utility grid. As Fig. 2.5 illustrates, the distribution feeder net load, which should be supplied by the utility grid, consists of several rampings in the order of a few MW/10-min as well as a severe ramping of 8.9 MW/10-min between hours 11 and 12. In Fig. 2.6, however, all these variabilities are reduced to 0.5 MW/10-min as targeted by the grid operator. Moreover, Fig. 2.7 depicts the ramping of the utility grid in both studied cases. This figure clearly demonstrates the effectiveness of the proposed model in reducing the distribution network net load ramping, as the obtained data from Case 2 is efficiently confined between the desired ramping values.

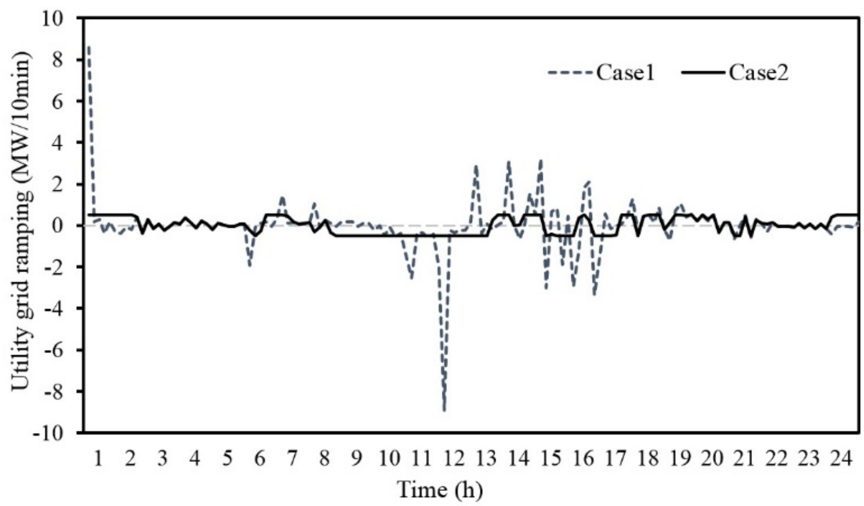

Fig. 2.7. Utility grid net load ramping in the two studied cases.

The results in Case 2 advocate that to obtain the desired ramping the microgrid needs to deviate from its price-based schedule. This deviation results in a \$328.7 increase in the microgrid operation cost (i.e., \$12,077–\$11,748.3). This increase represents the microgrid lost revenue. To incentivize the microgrid to opt in for offering flexibility services to the utility grid, the amount of incentive that should be paid to the microgrid must be equal to or greater than this amount. If less, the microgrid would prefer to find its price-based schedule while disregarding the grid requirements. However, it would be extremely beneficial for the utility grid to incentivize the microgrid, otherwise the microgrid may exacerbate the distribution network net load variability as discussed in Case

1. It is worth mentioning that the microgrid lost revenue is a function of the consumers/prosumers net load variations as well as values of Δ_1 and Δ_2 which are further investigated in the following.

Case 3: After proving the effectiveness of the proposed model by comparing Cases 1 and 2, the impact of ramping limits is studied in this case. To show that the microgrid is also capable of meeting tight ramping limits, a value of zero is considered for the intra-hour ramping and 2 MW/10-min for the inter-hour ramping. Fig. 2.8 depicts the solution of this case. Considering a value of zero for intra-hour ramping completely eliminates the intra-hour variabilities in the distribution network net load, hence the obtained consumption is constant within each operation hour while it can change by up to 2 MW between any two consecutive operation hours.

To closely follow the limits, the microgrid imported power from the utility grid is decreased when the net load is increasing. Furthermore, microgrid's export to the utility grid in high price hours is changed to support the ramping limits. For instance, the microgrid power export to the utility grid in hours 12-14, which was based on economic considerations, is now changed to power import from the utility grid. Fig. 2.9 shows the obtained results of Fig. 2.8 between hours 12 and 20, which better demonstrates the viable application of the microgrid in reducing the net load variability and sharp ramping.

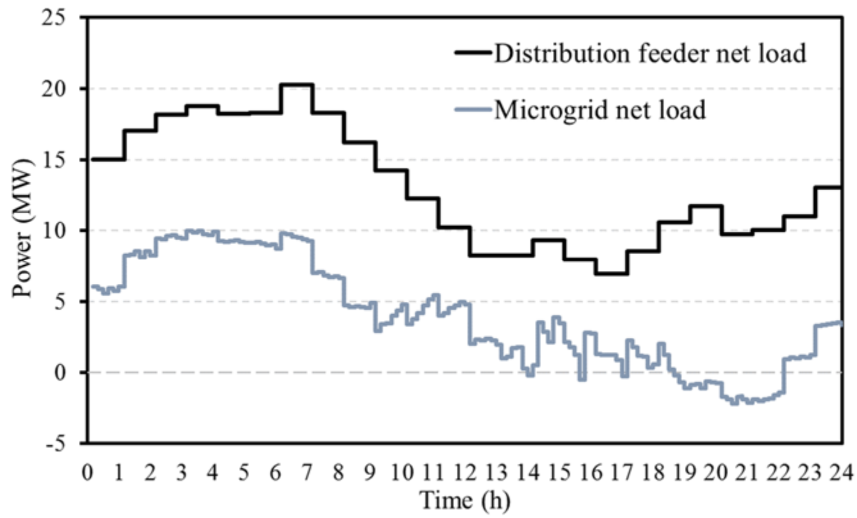

Fig. 2.8. Distribution feeder net load, and microgrid net load for 2 MW/10-min inter-hour and 0 MW/10-min intra-hour utility ramping.

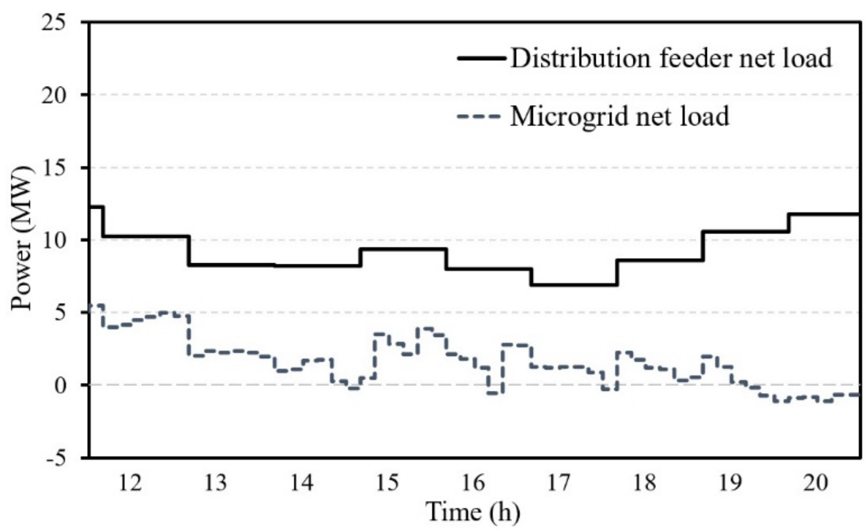

Fig. 2.9. Distribution feeder net load, and microgrid net load for 2 MW/10-min inter-hour and 0 MW/10-min intra-hour utility ramping, during net load peak hours.

The results of flexibility-oriented microgrid optimal scheduling for different amounts of inter-hour (changing between 0.5 and 5) and intra-hour (changing between 0 and 2) ramping limits are provided in Table 2.9. It should be noted that all obtained results are near-optimal, mainly due to nonlinearity of the original problem and presence of uncertainties.

Table 2.9 Microgrid Operation Cost ($) for Various Ramping Limits

Inter-hour ramping limit Δ_2 (MW/10min)	Intra-hour ramping limit Δ_1 (MW/10 min)			
	0	0.5	1	2
0.5	36305.6	12077.0	11886.9	11825.3
1	19799.1	12011.5	11860.1	11804.0
1.5	14930.4	11977.5	11845.2	11796.5
2	13329.1	11951.4	11834.1	11790.1
2.5	12790.2	11936.4	11826.4	11786.0
3	12607.5	11925.8	11819.7	11782.1
3.5	12532.5	11916.8	11813.7	11778.6
4	12485.9	11906.8	11808.6	11775.6
4.5	12460.1	11898.3	11804.3	11772.7
5	12445.6	11891.0	11800.1	11770.1

The obtained results show that the microgrid operation cost is increased by decreasing the inter-hour and intra-hour ramping limits, however these changes are not linear. For example, the microgrid operation cost when the intra-hour ramping limit is 0 is considerably higher than other cases. This is due to two main reasons: (i) the need to commit more units and dispatch them at uneconomical operation points, in a way that they can provide the required flexibility, and (ii) the possibility of load curtailment in the microgrid. The ramping limits are added as constraints to the problem, while the load curtailment is added as a penalty to the objective function. It results in prioritizing the flexibility limit (i.e., problem feasibility) on the load curtailment (i.e., problem optimality). There of course should be additional measures to consider in order to prevent load curtailment in the microgrid which are currently under investigation by the authors. The utility grid incentive in each case must at least cover the microgrid's lost revenue. According to Table 2.9, if the utility grid decides to eliminate the intra-hour ramping, it should pay at least $24,557.3 and $697.3 to the microgrid for Δ_2 values equal to 0.5 MW/10-min and 5 MW/10-min, respectively. Whereas, in the case of 2 MW/10-min as desired intra-hour ramping, at least \$77 and \$21.8 should be paid to the microgrid for Δ_2 equal to 0.5 MW/10-min and 5 MW/10-min, respectively. These results advocate for the importance of a cost-benefit analysis from the grid operator to determine the most suitable inter-hour and intra-hour ramping limits.

2.4 Discussions

Microgrids can potentially be utilized in distribution networks as a solution for mitigating net load ramping and variability. According to the studied cases in this chapter, the following features of the proposed microgrid optimal scheduling model with multi-period islanding and flexibility constraints, could be concluded:

- Flexibility consideration: The inter-hour and intra-hour ramping constraints have been considered in the proposed model to ensure that the utility grid desired power is obtained for different time resolutions.
- Economic and reliable operation: The proposed model determines the least-cost schedule of microgrid loads and DERs while supporting the utility grid in addressing net load ramping. In addition, the consideration of Θ-k islanding criterion ensures the microgrid reliability in supplying local loads during the islanded mode.
- High resolution scheduling: 10-minute time interval scheduling was considered in studied cases, which offers a high resolution scheduling and is efficient for capturing net load variabilities. The proposed model offers the capability to consider various intra-hour time resolutions.
- Localized and low-cost solution: Using microgrids as local solutions for addressing distribution net load ramping can significantly reduce the utility grid investments in

upgrading the generation, transmission, and distribution facilities. This significant cost saving would be made possible at the small expense of incentivizing microgrids to offer flexibility services.

3. Chapter Three: Providing Ancillary Services to the Utility Grid

The grid-connected operation mode of the microgrid is considered in this chapter, as the microgrid exchanges power with the utility grid and is able to manage its net load in support of the utility grid operation. Three time resolutions are considered in this study, including hourly (for ramping support), 10-minute based (for load following) and 1-minute based (for frequency regulation). A mixed-integer programming (MIP) model is used to formulate the microgrid optimal scheduling problem subject to prevailing operational and added flexibility constraints.

3.1 Ancillary Service Support Model Outline and Problem Formulation

The objective of the microgrid optimal scheduling problem is to minimize the microgrid operation cost (3.1) subject to constraints associated with load balance (3.2), utility power exchange (3.3), dispatchable DGs (2.9)-(2.15), energy storage (2.16)-(2.23), and adjustable loads (2.24)-(2.26), which were comprehensively explained in Chapter 2.

$$\min \sum_{t}\sum_{k}\tau\,[\sum_{i\in G}F(P_{itk})+\rho_{t}^{M}P_{tk}^{M}] \tag{3.1}$$

$$\sum_{i}P_{itk}+P_{tk}^{M}=\sum_{d}D_{dtk} \qquad \forall t,\forall k, \tag{3.2}$$

$$-P^{M,\max}\le P_{tk}^{M}\le P^{M,\max} \qquad \forall t,\forall k, \tag{3.3}$$

To enable grid support, intra-hour and inter-hour limits are further imposed on the utility power exchange as proposed in (3.4) and (3.5).

$$\Delta_{1,tk}^{low}\le P_{tk}^{M}-P_{t(k-1)}^{M}\le\Delta_{1,tk}^{up} \qquad \forall t,k\neq 1, \tag{3.4}$$

$$\Delta_{2,t}^{low} \le P_{t1}^{M} - P_{(t-1)K}^{M} \le \Delta_{2,t}^{up} \qquad \forall t. \tag{3.5}$$

The flexibility constraints are imposed to the microgrid optimal scheduling problem as restrictions on the microgrid power exchange with the utility grid. To understand how these limits will reflect utility grid requirements, (3.6)-(3.8) need to be considered:

$$P_{tk}^{u} = P_{tk}^{M} + \sum_{j\in N} P_{jtk}^{c} \qquad \forall t, \forall k, \tag{3.6}$$

$$\left| P_{tk}^{u} - P_{t(k-1)}^{u} \right| \le \Delta_1 \qquad \forall t,\ k \ne 1, \tag{3.7}$$

$$\left| P_{t1}^{u} - P_{(t-1)K}^{u} \right| \le \Delta_2 \qquad \forall t, \tag{3.8}$$

where P^u represents the feeder net load which should be supplied by the utility grid, P^M represents the microgrid net load, and P_j^c represents the net load of each consumer/prosumer in the feeder. In order to eliminate the net load variability seen by the utility grid, the intra-hour and inter-hour variability limits, as represented in (3.7) and (3.8), need to be satisfied. The utility grid flexibility limits, Δ_1 and Δ_2, are constant and determined by the grid operator to achieve the desired net load in the distribution network. By substituting P_{tk}^u in constraints (3.7) and (3.8) by its equivalent from (3.6) and rearranging the terms, the utility grid flexibility limits can be converted into limits on the microgrid net load as proposed in (3.4) and (3.5) and determined as follows:

$$\Delta_{1,tk}^{low} = -\Delta_1 - \Big(\sum_{j\in N} P_{jtk}^{c} - \sum_{j\in N} P_{jt(k-1)}^{c}\Big) \qquad \forall t, k \ne 1, \tag{3.9}$$

$$\Delta_{1,tk}^{up} = \Delta_1 - \Big(\sum_{j\in N} P_{jtk}^{c} - \sum_{j\in N} P_{jt(k-1)}^{c}\Big) \qquad \forall t,\ k \ne 1, \tag{3.10}$$

$$\Delta_{2,t}^{low} = -\Delta_2 - \Big(\sum_{j\in N} P_{jt1}^{c} - \sum_{j\in N} P_{j(t-1)K}^{c}\Big) \qquad \forall t, \tag{3.11}$$

$$\Delta_{2,t}^{up} = \Delta_2 - \Big(\sum_{j\in N} P_{jt1}^{c} - \sum_{j\in N} P_{j(t-1)K}^{c}\Big) \qquad \forall t. \tag{3.12}$$

As (3.9)-(3.12) demonstrate, the obtained boundaries of microgrid flexibility constraints are variable due to the inclusion of the aggregated net load of all consumers/prosumers in the distribution feeder. Thus, although Δ_1 and Δ_2, as the utility grid flexibility limits, are constant and determined by the grid operator to achieve the desired net load in the distribution network, the limitations of (3.4) and (3.5) are functions of *t* and *k* and vary with high resolutions. As the upper and lower limits of these constraints change for different time resolutions (that is various *k* values), the offered services by the microgrid will change, which will be discussed subsequently for ramping, load following, and frequency regulation services. Fig. 3.1 depicts the flowchart of the proposed model. It should be noted that the proposed model is generic and can be applied to any microgrid independent of its size [84].

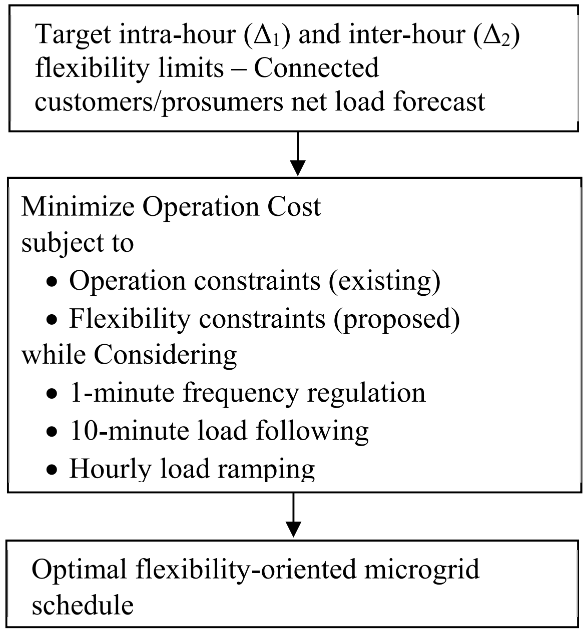

Fig. 3.1. Flowchart of the proposed model.

3.1.1 Microgrid to Support 1-Minute Frequency Regulation

To offer frequency regulation services, the resolution of the microgrid's DERs generation and loads, net load of distributed consumers/prosumers, as well as the power supply of utility grid to the feeder should be considered as one minute. The unit commitment can still be determined hourly and the scheduling problem will be solved for the 24-hour scheduling horizon. Therefore, t and k would be in the intervals of $1<t<24$ and $1<k<60$ as the inter-hour and intra-hour time indices, respectively.

3.1.2 Microgrid to Support 10-Minute Load Following

A 10-minute flexibility for the microgrid power dispatch in order to mitigate the variation of distribution feeder net load would offer a load following service. The resolution of net load of distributed consumers/prosumers, as well as the power supply of the utility grid to the feeder can still be considered in the one-minute resolution. So, the intra-hour time index k' is defined for microgrid ($1 < k' < 6$), while other time indices (t and k) are the same as in frequency regulation. In this case the microgrid power dispatch would vary every 10 minutes to capture the intra-hour ramping of the distributed net load, while it has the fixed power dispatch during each 10-minute time interval.

3.1.3 Microgrid to Support Hourly Ramping

To offer hourly ramping services, the microgrid dispatches the power hourly to mitigate the ramping of distribution feeder net load. The resolution of net load of distributed consumers/prosumers, as well as the power supply of the utility grid to the feeder is still one minute, same as other services. In this case variable k should be deleted from the objective function and constraints, since the resolution of the microgrid dispatch is one hour, i.e., no intra-hour time period is required for the microgrid dispatch. Accordingly, the intra-hour flexibility constraint will be relaxed and just the inter-hour flexibility constraint (3.5) will be imposed to the scheduling model.

3.1.4 Microgrid with Limited Flexibility

Although by imposing the proposed flexibility constraints the microgrid is capable of providing ancillary services to the utility grid, it is always possible that the microgrid does not have the capability to fully address the utility grid requirement, i.e., the adequate ramping is not available to be offered to the utility grid. Therefore, the major limitation of the proposed model results from the microgrid's limited capability in offering the aforementioned services. This limitation is caused based on the characteristics of the microgrid resources. In cases where the microgrid does not have adequate flexibility for supporting the utility grid, the maximum available flexibility is provided and any required flexibility beyond this limit is covered by the utility grid, i.e., the utility grid should pick up the remaining flexibility that could not be provided by the microgrid. This inadequacy, however, would result in an infeasible solution considering the added flexibility constraints. To address this issue while calculating the amount of remaining flexibility that the utility grid needs to provide, the flexibility constraints are revised as follows using nonnegative slack variables SL_1 and SL_2:

$$\Delta_{1,tk}^{low} \le P_{tk}^{M} - P_{t(k-1)}^{M} + SL_{1,tk} - SL_{2,tk} \le \Delta_{1,tk}^{up} \qquad \forall t, k \ne 1, \tag{3.11}$$

$$\Delta_{2,t}^{low} \le P_{t1}^{M} - P_{(t-1)K}^{M} + SL_{1,t} - SL_{2,t} \le \Delta_{2,t}^{up} \qquad \forall t. \tag{3.12}$$

The value of these slack variables in different time periods show the amount of variations beyond utility grid desired flexibility which cannot be captured by the microgrid and should be addressed by the utility grid. In order to minimize the value of slack variables, which accordingly leads to leveraging the maximum possible microgrid flexibility for supporting the utility grid, the summation of slack variables will be penalized in the objective function using a large positive penalty factor.

3.2 Numerical Simulations

The objective of A microgrid with four dispatchable units, two non-dispatchable units including wind and solar, one energy storage, and five adjustable loads is used for studying the performance of the proposed models. The characteristics of the DERs and loads (adjustable and fixed), and the hourly market price are borrowed from [83] and are tabulated in Tables 2.1 -2.6. Fig. 3.2 shows the generation profile of nondispatchable units with a 1-minute resolution. Fig. 3.3 depicts the aggregated net load of consumers/prosumers connected to the distribution feeder.

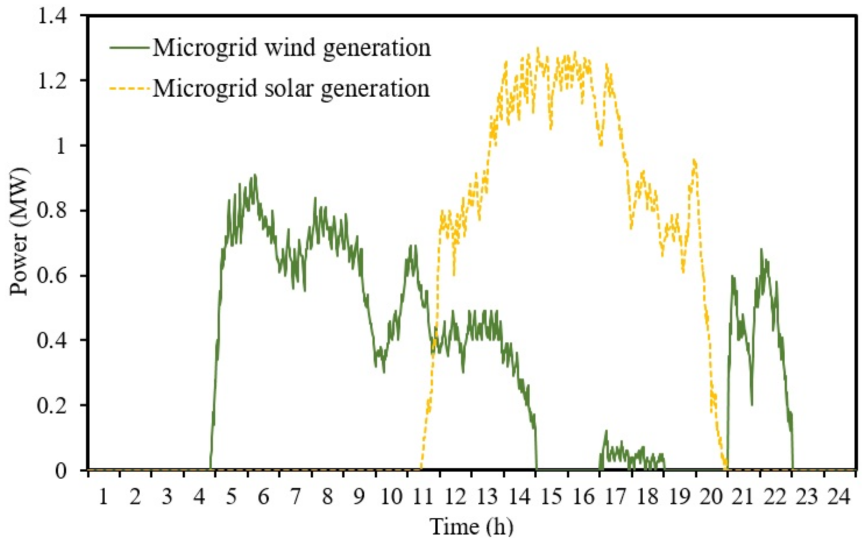

Fig. 3.2. Nondispatchable units' generation.

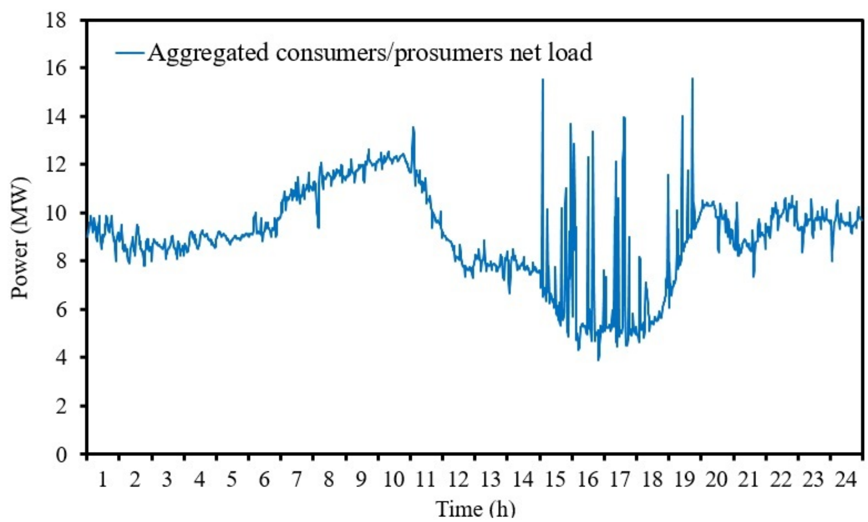

Fig. 3.3. Aggregated consumers/prosumers net load in the distribution feeder.

The capacity of interconnection line between the microgrid and the utility grid is assumed to be 10 MW. The developed mixed-integer programming models are solved using CPLEX 12.6 by a high-performance computing server consisting of four 10-core Intel Xeon E7-4870 2.4 GHz processors.

The following five cases are studied in this chapter:

Case 1: Price-based optimal scheduling (ignoring flexibility constraints).

Case 2: Flexibility oriented scheduling for frequency regulation.

Case 3: Flexibility oriented scheduling for load following.

Case 4: Flexibility oriented scheduling for hourly ramping.

Case 5: Investigating the proposed model validity for a larger microgrid.

Case 1: The price-based microgrid optimal scheduling problem with one minute resolution is solved for a 24-hour horizon in this case. Under price-based scheduling conditions, the microgrid does not have any commitment to support the utility grid in mitigating distribution network net load ramping, where the minimization of the operation cost is the microgrid's priority. The utility grid would be responsible for capturing the distribution net load ramping illustrated in Fig. 3.4 in this case. As this figure shows, the aggregated net load consists of considerable changes, especially the sharp ramps between hours 14 and 19, due to severe variations of solar generation in these hours, which in some cases are as high as 8 MW/min. Fig. 3.4 depicts the effect of considering microgrid in the distribution feeder without any commitment to the utility grid.

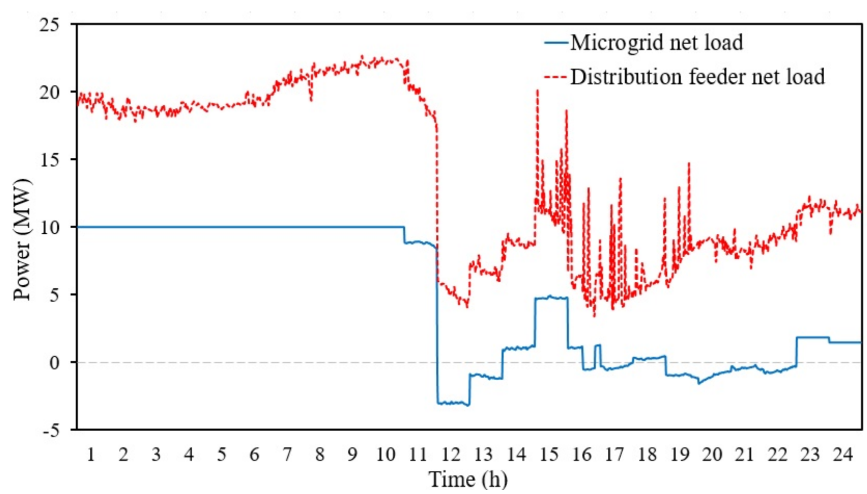

Fig. 3.4. Distribution feeder and microgrid net loads for the 24-hour scheduling horizon in Case 1.

As Fig. 3.4 shows, the microgrid imports power from the utility grid in low price hours while switches over to local generation and exports power to the utility grid in high price hours. This scheduling increases utility grid power in hours 1- 11 and results in a 22.65 MW peak load in hour 9, as a new morning peak, for this distribution network. In addition, it increases the number of sharp ramps and exacerbates the distribution network net load variability. The microgrid operation cost in this case is $11,311.

Case 2: In this case, the flexibility-oriented microgrid optimal scheduling along with 1-minute load following is solved. The values of 0 MW/min and 2 MW/h are considered for intra-hour and inter-hour flexibility limits, respectively. Fig. 3.5 shows the distribution feeder net load and the microgrid net load. This figure illustrates that how the microgrid can effectively capture net load variabilities. The intra-hour flexibility limit is 0 MW/min, so the microgrid net load is changed every minute to capture the feeder net load variabilities.

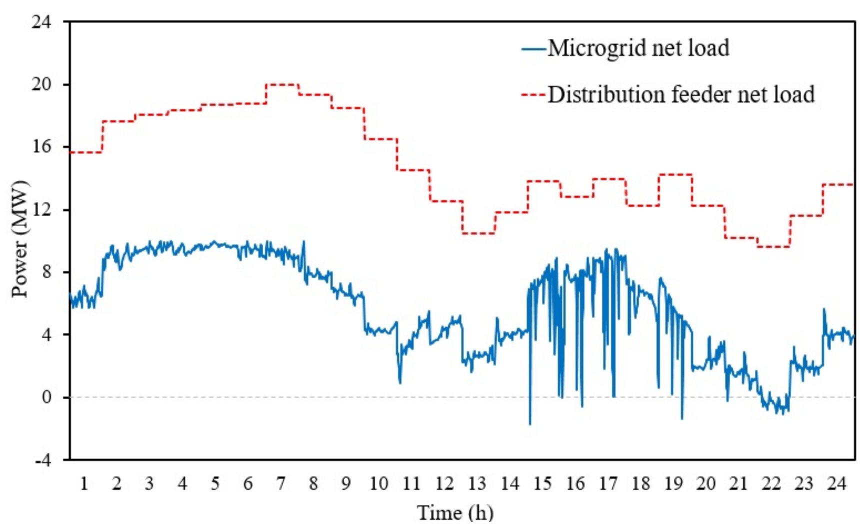

Fig. 3.5. Distribution feeder and microgrid net loads for 0 MW/min intra-hour and 2 MW/h inter-hour utility ramping in Case 2.

The microgrid net load variations are particularly high during evening hours when used to capture the distributed solar generation variabilities. The distribution feeder net load seen by the utility grid in this case is constant during each one hour period and its inter-hour ramping is limited to 2 MW/h.

Fig. 3.6 shows the obtained results of Fig. 3.5 in the extreme fluctuation period, i.e., between hours 12 and 21, which better demonstrates the positive impact of the microgrid in eliminating the net load variability and support in frequency regulation. Consideration of ramping constraints leads to an increase in the microgrid operation cost to $12971, i.e., a 14.7% increase compared to that of Case 1. This increase in the microgrid operation cost, which represents a lost revenue, should be paid to the microgrid as an incentive for the contribution in supporting the utility grid. If the microgrid is not incentivized or paid less than this amount, it would be more economical to operate on a price-based basis (Case 1), without any commitment to the utility grid.

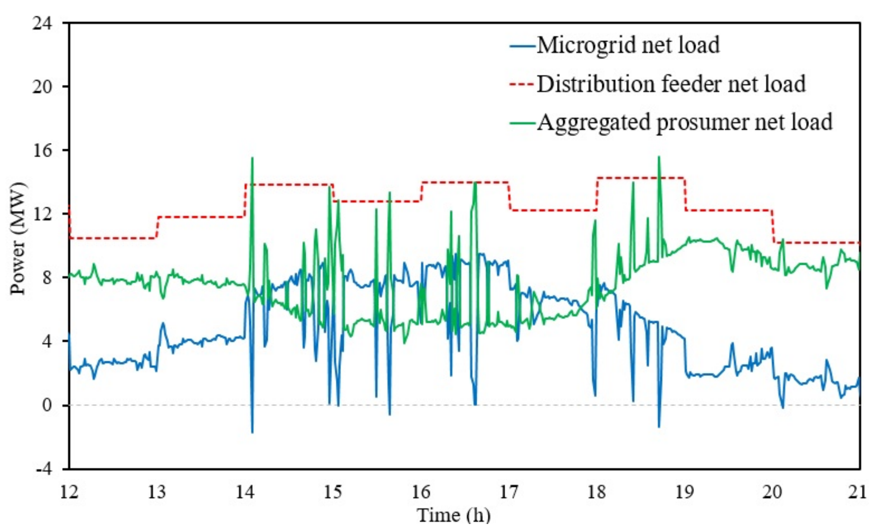

Fig. 3.6 Aggregated consumers/prosumers, distribution feeder, and microgrid net loads for 0 MW/min intra-hour and 2 MW/h inter-hour utility ramping, during net load high fluctuation hours in Case 2.

Case 3: In this case, the flexibility-oriented microgrid optimal scheduling with 10-minute load following is solved. In order to enable a reasonable comparison with other cases, 2/60 MW/min is considered for intra-hour ramping limit (Δ_1) which equals to 2 MW ramping capability in one hour. In addition, 2 MW/h is considered for inter-hour ramping limit (Δ_2) in this case. Fig. 3.7 depicts the obtained results of the microgrid and the distribution feeder net loads. As the figure shows, the microgrid power dispatch is constant in each 10-minute period and the higher resolution variabilities of aggregated consumers/prosumers net load are captured by the utility grid. Since the microgrid power dispatch is fixed in 10-minute time intervals, and the intra-hour ramping of the utility grid is restricted to 2/60 MW/min, the variations more than this amount in each 10-minute interval will appear in slack variables. The inter-hour variations more than 2 MW/h are captured by the microgrid and the variations beyond microgrid ramping capability are also covered by slack variables.

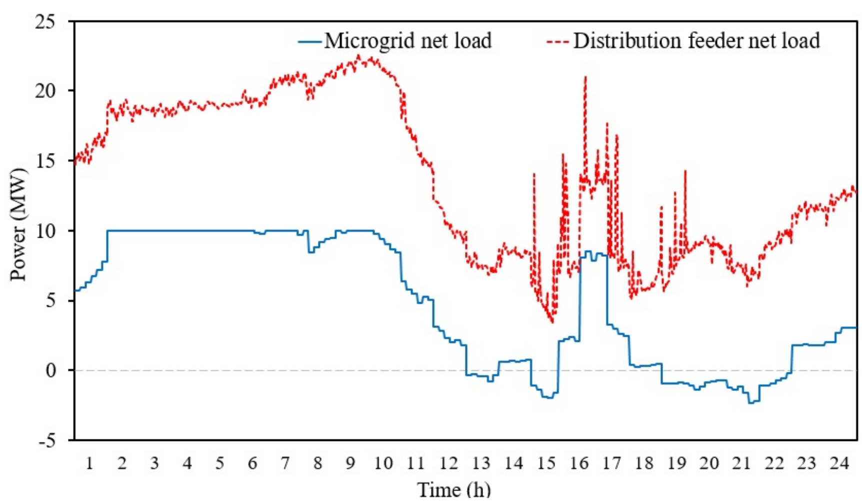

Fig. 3.7. Distribution feeder and microgrid net load for 0.033 MW/min intra-hour and 2 MW/h inter-hour utility ramping, in case 3.

The microgrid operation cost in this case is calculated as \$12149. The 7.3% increase in the microgrid operation cost should be paid to the microgrid as an incentive for the contribution in mitigating the distribution network net load variability.

Case 4: In this case, the flexibility-oriented microgrid optimal scheduling along with hourly load following is solved to support the utility grid in addressing net load ramping. A 2 MW/h is considered for inter-hour ramping limit, while there will be no need to consider the intra-hour ramping limit. Fig. 3.8 depicts the distribution feeder net load and the microgrid net load in this case. As this figure shows, the variations of the aggregated consumers/prosumers net load are captured by the utility grid since the microgrid follows the load hourly, unlike Case 2 in which the microgrid followed the load on a 1-minute basis. However, the ramping of the distribution net load is controllable by changing the inter-hour ramping constraint, which is defined by the utility grid. The microgrid operation cost in this case is \$11476, which shows a 1.9% increase compared to that of Case 1.

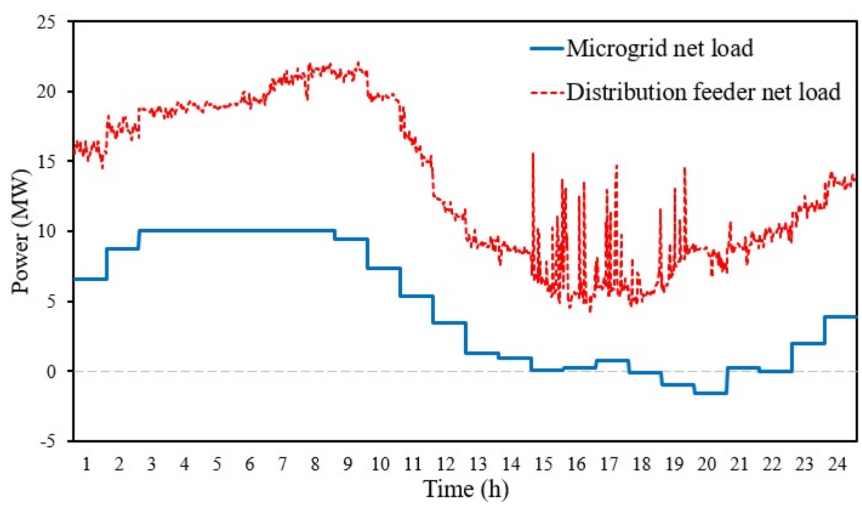

Fig. 3.8. Distribution feeder and microgrid net loads for 2 MW/h inter-hour utility ramping in Case 4.

A comparison between Fig. 3.8 and Fig. 3.5 shows that hourly ramping (Case 4) is not as effective as the 1-minute frequency regulation (Case 2) in capturing the distribution network net load variabilities. However, there is a trade-off between the effectiveness of the offered service and the microgrid operation cost. The obtained results show that the microgrid operation cost in Case 2 is almost 14.7% more than price-based optimal scheduling, while the microgrid operation cost in Case 4 is just about 1.9% greater than that of Case 1. The standard deviation of distribution feeder net load variabilities (i.e., the standard deviation of ramping) has been defined as an index for illustrating the reduction in variabilities. Fig. 3.9 depicts the standard deviation of distribution feeder net load variabilities versus microgrid operation cost for all four studied cases. The figure presents that Case 1 has the highest amount of standard deviation owing to ignoring flexibility constraints, while Case 2 (frequency regulation) has the lowest amount of variability standard deviation as it closely follows the feeder net load and captures variabilities. This figure further demonstrates the trade-off between the effectiveness of the offered service and the microgrid operation cost. The cases with the lower amount of variabilities in distribution feeder net load have higher microgrid operation cost and vice versa. An accurate cost-benefit analysis should be performed by the grid operator in order to determine the value of each offered service to the system based on the associated variability limit.

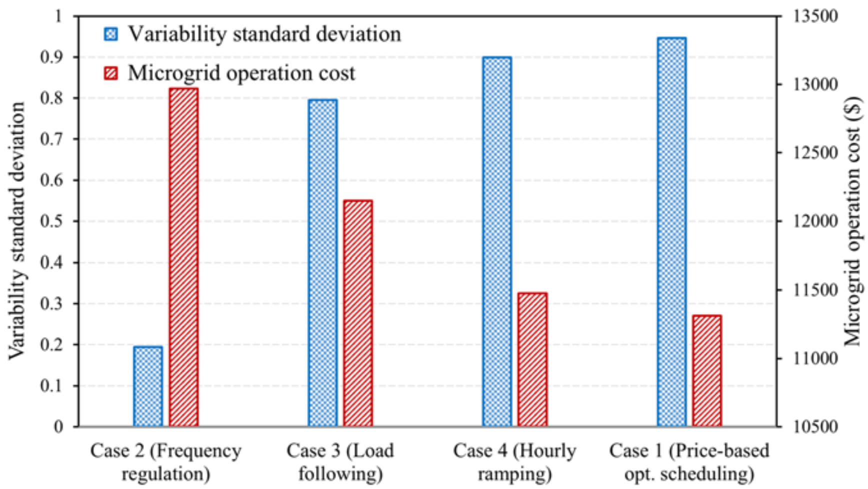

Fig. 3.9. Standard deviation of distribution feeder net load variabilities versus microgrid operation cost for studied cases.

Case 5: In order to illustrate the effectiveness of the proposed model in offering the mentioned services to the utility grid for different microgrids, a larger microgrid is studied in this case. The studied microgrid consists of twelve dispatchable units and fifteen adjustable loads (repeated from previous cases). The total fixed load is also borrowed from the previous case and multiplied by three to represent a larger microgrid. The peak load for this microgrid is 48.42 MW and the total installed dispatchable capacity is 48 MW.

The obtained results show that this microgrid properly provides frequency regulation services to the utility grid similar to Case 2. However, the microgrid operation cost is increased to $37,343, owing to providing the power to a larger load. The computation time is increased to 265 s from 11.9 s in Case 2. This is expected as the problem to be solved is considerably larger than that in Case 2 and includes many more variables and parameters. Moreover, this microgrid offers the capability to serve a higher amount of flexibility to the utility grid (i.e., for lower amounts of Δ_2). One important issue to consider here is that a day-ahead scheduling problem is solved, i.e., for the 24 hours of the next day with minute intervals, therefore the increase in the computation time will not impact the viability of the proposed model.

This microgrid is further studied for load following and hourly ramping, where the microgrid operation cost and computation time are respectively obtained as \$37,254 and 21.3 s in the former and \$36,120 and 1 s in the latter. Fig. 3.10 depicts standard deviation of distribution feeder net load variabilities versus microgrid operation cost for various ancillary services to the utility grid in this case. Comparison of Figs. 3.9 and 3.10 demonstrates that the trade-off between microgrid operation cost and variability of distribution feeder for both sizes of microgrid is almost the same. However, it should be noted that the larger microgrid significantly increases distribution feeder variability when operating in price-based optimal scheduling, i.e. no considering flexibility constraints, and it has much more negative impact on the load profile of distribution feeder compared with existing of smaller microgrid in the feeder.

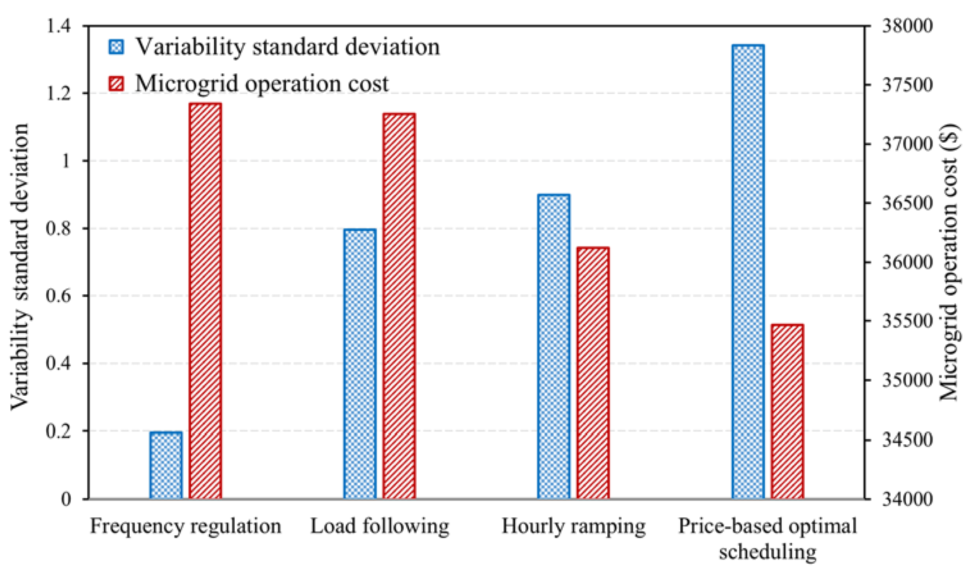

Fig. 3.10. Standard deviation of distribution feeder net load variabilities versus microgrid operation cost for various ancillary services to the utility grid in Case 5.

But since the flexibility limits in Case 5 is the same as other cases, variability standard deviation in frequency regulation, load following, and hourly ramping in both Figs. 3.9 and 3.10 are almost the same. These results advocate that the proposed model can effectively handle larger microgrids, at the expense of increased computation time. If required, available decomposition techniques such as Benders decomposition can be applied to the proposed model to decompose the large-scale problem into smaller and easier to solve subproblems, and thus, significantly reduce the computation time. The decomposition process for large-scale power system problems has been extensively investigated by the authors in their previous works [85], [86].

3.4 Discussions

- In this chapter a flexibility-oriented microgrid optimal scheduling model was proposed to efficiently schedule microgrid resources to support utility grid operation via providing ancillary services.
- The proposed model considered intra-hour and inter-hour time intervals during the 24-hour day-ahead scheduling horizon, offering 1-minute frequency regulation service, 10-minute load following service, and hourly ramping service.
- The numerical results confirmed the effectiveness of the proposed model in various cases, and further advocated that higher resolution services, such as frequency regulation, could lead to smoother distribution net load profiles while causing higher operation costs.
- The microgrid lost revenue, that should be paid by the utility grid to microgrid as a compensation and/or incentive, is a function of the consumers/prosumers net load

variations as well as desired values of the utility grid's ramping limits which needs to be calculated using additional cost-benefit analyses.

4. Chapter Four: Capturing Uncertain Distribution Network Net-Load Ramping

Unlike the conventional energy resources, renewable generation is inherently variable (generation constantly varies) and uncertain (generation cannot be forecasted with perfect accuracy) [87]. The studies by the North American Electric Reliability Corporation (NERC) show that the power generation of solar panels can change by ±70%, in a timeframe of 2–10 minutes, several times per day, in addition to the typical ±1% to ±7% deviation between predicted demand and actual demand in the system [87]. The high penetration of renewable generation has significantly increased the system uncertainty which further challenges traditional methods in cost-effective and reliable control, operation, and planning of power systems [88], [89]. Therefore, uncertainty considerations in power system operation and planning have been significantly increased in the past few years [79], [85], [87], [90]–[93].

Leveraging potential flexibility of existing microgrids in distribution networks as a local, novel, and viable method was proposed in previous chapters and extended in this chapter to address aforementioned challenges and to alleviate the negative impacts of increasing renewable penetration. A flexibility-oriented microgrid optimal scheduling under uncertainty is proposed in this chapter to address distribution network net load ramping. The robust optimization method is used for capturing uncertainties and increasing the practicality of the proposed model.

4.1 Problem Modeling and Formulation

4.1.1 Problem Statement

The power (P^u) that the electric utility should supply to a certain distribution feeder is equal to the microgrid net load (P^M) plus the aggregated net load of other customers, including consumers and prosumers, in this feeder (P^c) as presented in (4.1).

$$P_t^u = P_t^M + \sum_{j \in N} P_{jt}^c \qquad \forall t. \tag{4.1}$$

The net load of consumers and prosumers is highly variable and uncertain, primarily due to the deployment of distributed renewable energy resources, and is further uncontrollable from the utility side. The net load of the microgrid, moreover, is controlled by the microgrid controller based on economy and reliability considerations. The summation of these two uncontrollable net loads with considerable levels of renewable generation causes variability (mainly in terms of large ramps) and uncertainty for the power that the electric utility needs to provide. A viable solution, however, is to incentivize the microgrid to locally capture the ramping, i.e., not only the microgrid retracts its variability, but also helps the electric utility in capturing the variability of other customers connected to the same distribution feeder. To model this, the utility grid ramping limit (4.2) should be translated into proper limitations on the microgrid net load as discussed in the next subsection.

$$\left| P_t^u - P_{(t-1)}^u \right| \le \Delta \qquad \forall t. \tag{4.2}$$

4.1.2 Problem Formulation

The flexibility-oriented microgrid optimal scheduling model under uncertainty is proposed as in (4.3)-(4.21).

$$\max_{U} \min_{P} \sum_{t} [\sum_{i \in G} F(P_{it}) + \rho_t^M P_t^M] \tag{4.3}$$

$$\sum_{i} P_{it} + P_t^M = \sum_{d} D_{dt} \qquad \forall t, \tag{4.4}$$

$$-P^{M,\max} \le P_t^M \le P^{M,\max} \qquad \forall t, \tag{4.5}$$

$$P_i^{\min} I_{it} \le P_{it} \le P_i^{\max} I_{it} \qquad \forall i \in G, \forall t, \tag{4.6}$$

$$P_{it} - P_{i(t-1)} \le UR_i \qquad \forall i \in G, \forall t, \tag{4.7}$$

$$P_{i(t-1)} - P_{it} \le DR_i \qquad \forall i \in G, \forall t, \tag{4.8}$$

$$T_{it}^{on} \ge UT_i (I_{it} - I_{i(t-1)}) \qquad \forall i \in G, \forall t, \tag{4.9}$$

$$T_{it}^{off} \ge DT_i (I_{i(t-1)} - I_{it}) \qquad \forall i \in G, \forall t, \tag{4.10}$$

$$P_{it} \le P_{it}^{dch,\max} u_{it} - P_{it}^{ch,\min} v_{it} \qquad \forall i \in S, \forall t, \tag{4.11}$$

$$P_{it} \ge P_{it}^{dch,\min} u_{it} - P_{it}^{ch,\max} v_{it} \qquad \forall i \in S, \forall t, \tag{4.12}$$

$$u_{it} + v_{it} \le 1 \qquad \forall i \in S, \forall t, \tag{4.13}$$

$$C_{it} = C_{i(t-1)} - (P_{it} u_{it} \tau / \eta_i) - P_{it} v_{it} \tau \qquad \forall i \in S, \forall t, \tag{4.14}$$

$$C_i^{\min} \le C_{itks} \le C_i^{\max} \qquad \forall i \in S, \forall t, \forall k, \forall s, \tag{4.15}$$

$$T_{it}^{ch} \ge MC_i (u_{it} - u_{i(t-1)}) \qquad \forall i \in S, \forall t, \tag{4.16}$$

$$T_{it}^{dch} \ge MD_i (v_{it} - v_{i(t-1)}) \qquad \forall i \in S, \forall t, \tag{4.17}$$

$$D_{dt}^{\min} z_{dt} \le D_{dt} \le D_{dt}^{\max} z_{dt} \qquad \forall d \in D, \forall t, \tag{4.18}$$

$$T_d^{on} \ge MU_d (z_{dt} - z_{d(t-1)}) \qquad \forall d \in D, \forall t, \tag{4.19}$$

$$\sum_{t \in [\alpha_d, \beta_d]} D_{dt} = E_d \qquad \forall d \in D, \tag{4.20}$$

$$\Delta_t^{low} \le P_t^M - P_{(t-1)}^M \le \Delta_t^{up} \qquad \forall t. \tag{4.21}$$

The objective of this problem is to minimize the microgrid operation cost over primary variables and to maximize over uncertain variables. The microgrid operation cost consists of two terms; local generation cost, i.e. the first term of (4.3), and the cost of power exchange with the utility grid, i.e. the second term of (4.3). It should be noted that the primary variables are local DERs, loads, and utility grid power exchange, while uncertain variables are the net load of aggregated customers and the electricity price. Thus, a robust solution (i.e., the worst-case) will be calculated which ensures that the microgrid can capture distribution network net load ramping even if load, generation, and price forecasts are uncertain.

This objective is subject to system constraints (4.4)-(4.5), component constraints (4.6)-(4.20), and the flexibility constraint (4.21). The load balance equation (4.4) ensures that adequate generation is available (locally and purchased from the utility grid) to supply local loads. The capacity of the line connecting the microgrid to the utility grid defines the restriction on the exchanged power (4.5). Dispatchable units are subject to minimum and maximum generation capacity limits (4.6), ramping limits (4.7)-(4.8), and minimum up/down time limits (4.9)-(4.10). Constraints (4.11)-(4.17) define the restrictions on energy storage. The maximum and minimum amounts of charging and discharging are defined by (4.11) and (4.12). Constraint (4.13) checks the energy storage operation mode to ensure that it does not operate at both charging and discharging modes simultaneously. Available energy at each hour is calculated with (4.14), while its limitations are defined in (4.15). Constraints (4.16) and (4.17) specify the minimum charging and discharging time limits, respectively. Constraints (4.18)-(4.20) define the restrictions on adjustable loads, including rated power limitations (4.18), the minimum operating time (4.19), and the required energy to complete an operating cycle (4.20) [94]. Constraint (4.21) is the utility ramping limit which is translated into a constraint on the microgrid net load. This constraint is obtained by substituting the value of the utility power from (4.1) in (4.2) and rearranging the terms. The lower and upper limits, which now are functions of time, are calculated based on the net load of connected customers as in (4.22) and (4.23):

$$\Delta_t^{low} = -\Delta - (\sum_j P_{jt}^c - \sum_j P_{j(t-1)}^c) \qquad \forall t, \tag{4.22}$$

$$\Delta_t^{up} = \Delta - (\sum_j P_{jt}^c - \sum_j P_{j(t-1)}^c) \qquad \forall t. \tag{4.23}$$

4.1.3 Solution Approach

The proposed robust model is decomposed into a master problem and a subproblem using Benders decomposition as illustrated in Fig. 4.1. The master problem calculates the minimum operation cost considering only constraints that include binary variables. It can be represented as follows:

$$\min_P \sum_t \sum_{i \in G} F(P_{it}) \tag{4.24}$$

subject to (4.6), (4.9)-(4.13), (4.16)-(4.19).

Once binary scheduling variables are determined, including the DERs and loads schedules, these variables are sent to the subproblem, defined as follows:

$$\max_U \min_P \sum_t \rho_t^M P_t^M \tag{4.25}$$

subject to (4.4)-(4.8), (4.11)-(4.12), (4.14)-(4.15), (4.18), (4.20)-(4.21), and given binary variables from the master problem.

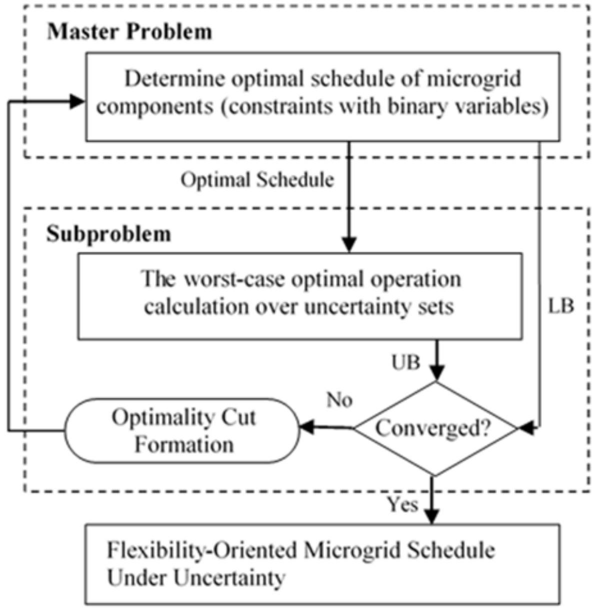

Fig. 4.1 Flowchart of the proposed flexibility-oriented microgrid optimal scheduling model.

The subproblem finds the microgrid's worst-case minimum operation cost over uncertainty sets based on the fixed schedules from the master problem. Since there is no binary variable in the subproblem, it is possible to convert the inner minimization problem into a maximization problem via duality theory and further combine the two maximization problems. Each uncertain parameter varies in an interval which is obtained from the forecasted value and expanded around the forecasted value based on the forecast error (i.e., a polyhedral uncertainty set). The robust optimization method finds the worst-case optimal operation solution while uncertain parameters vary within their associated uncertainty intervals. In order to control the robustness and restrict the solution conservatism, the budget of uncertainty is defined for confining the numbers of uncertain parameters which can take their worst-case values [85].

This robust optimization approach integrates uncertainties of distributed load, distributed solar generation, and market price forecasts. Once solved, the optimal DERs and loads schedules will be obtained which also ensure flexibility. Checking the lower and upper bound proximity of the problem is an approach for examining the solution convergence. As it is shown in the Fig. 4.1, the lower and the upper bounds of the problem are calculated in the master problem and the subproblem, respectively. The optimality cut will be formed in the subproblem and sent back to the master problem for updating the current schedule, if the solution is not converged. This iterative process continues until the convergence criterion is met and the solution is proven optimal [85].

4.2 Numerical Simulations

The microgrid used for studying the performance of the proposed model in this chapter consists of two nondispatchable units (solar and wind), four dispatchable units, one energy storage, and five adjustable loads. The characteristics of these energy resources, loads, as well as the hourly market price are available in [83] and are listed in Tables 2.1 – 2.6. The amount of aggregated load and solar generation in distribution feeder are tabulated in Tables 4.1 and 4.2, respectively. A 10 MW capacity is assumed for the line between the microgrid and the utility grid. The developed mixed-integer programming problems are solved using CPLEX 12.6.

Table 4.1 Aggregated Distributed Load

Time (h)	1	2	3	4	5	6
Load (MW)	13.50	12.50	11.80	11.70	12.10	12.50
Time (h)	7	8	9	10	11	12
Load (MW)	12.80	14.00	14.60	15.20	16.00	17.00
Time (h)	13	14	15	16	17	18
Load (MW)	18.50	18.00	17.00	16.70	17.00	18.00
Time (h)	19	20	21	22	23	24
Load (MW)	20.25	20.65	19.00	17.00	14.50	13.80

Table 4.2 Aggregated Distributed Solar Generation

Time (h)	1	2	3	4	5	6
Power (MW)	0.00	0.00	0.00	0.00	0.00	0.00
Time (h)	7	8	9	10	11	12
Power (MW)	0.00	0.00	1.00	4.00	8.00	11.50
Time (h)	13	14	15	16	17	18
Power (MW)	14.00	14.20	14.00	12.40	11.00	6.00
Time (h)	19	20	21	22	23	24
Power (MW)	2.75	0.85	0.00	0.00	0.00	0.00

Three cases are studied to show the effectiveness of the proposed model for addressing distribution network flexibility concerns:

- **Case 1:** Flexibility-oriented microgrid optimal scheduling ignoring uncertainty.
- **Case 2:** Flexibility-oriented microgrid optimal scheduling considering uncertainty.
- **Case 3:** Sensitivity analysis with regards to the budget of uncertainty.

Case 1: The flexibility-oriented microgrid optimal scheduling without consideration of any uncertainty is solved for a 24-hour horizon. The microgrid should capture the rampings above desired amount of the utility grid, which has been assumed as 2 MW/h in this case. When there is no contribution from the microgrid, the utility grid should capture the ramping of distribution feeder net load, for instance a maximum of 6 MW/h load change or an average of 4.6 MW/h in 3 hours. In this condition, unit 1 is ON for the entire 24 hours and commitment of other units changes to achieve the optimal operation. The operation cost is calculated as $11,262.8.

The comparison of distribution feeder net load with and without considering ramping constraint shows that in the case which there is no collaboration between the microgrid and the utility grid, i.e. no ramping constraints, even sharper ramps should be addressed by the utility grid. Indeed, in this case the microgrid exacerbated the distribution feeder net load variability, which should be supplied by the utility grid. The results show that in the absence of microgrid, the utility grid should address a maximum of 6 MW/h load change, or an average of 4.6 MW/h in 3 hours, while adding the microgrid in the feeder without consideration of any ramping constraints increases this amount to a maximum of 11.85 MW/h, or an average of 7 MW/h in 3 hours.

It is worthwhile to mention that the microgrid operation cost without consideration of any flexibility constraint is $11262.8, while it would be increased to $12126.3 after the addition of the ramping constraint. The reason of this cost increase, which should be paid to the microgrid by the utility grid, is the additional constraint that is imposed to the microgrid scheduling problem.

Case 2: The flexibility-oriented microgrid optimal scheduling considering prevailing uncertainties is solved for a 24-hour horizon. Forecast errors in distribution feeder load, solar generation, and market prices are considered as ±10%, ±20%, and ±10%, respectively. Furthermore, a 12-hour/day budget is considered as a limitation on uncertainty. A ramping limit of 2 MW/h is considered similar to Case 1.

Fig. 4.2 depicts the distribution feeder net load with and without considering flexibility constraint for ±10% load forecast error. As this figure shows, the utility grid encounters an average of 8.1 MW/h in 3 hours load change between hours 9 and 12 (maximum of 13.55 MW/h), as well as an average of 7.3 MW/h in 2 hours between hours 18 and 19 (maximum of 8 MW/h). The microgrid, however, restricts the ramping of the distribution feeder net load to 2 MW/h which has been requested by the utility grid. To obtain the desired ramping, the microgrid needs to deviate from its optimal schedule which leads to a $1,652.9 increase in its operation cost. This 14.7% increase in the microgrid operation cost should be paid by the electric utility as an incentive for contribution in mitigating the net load ramping.

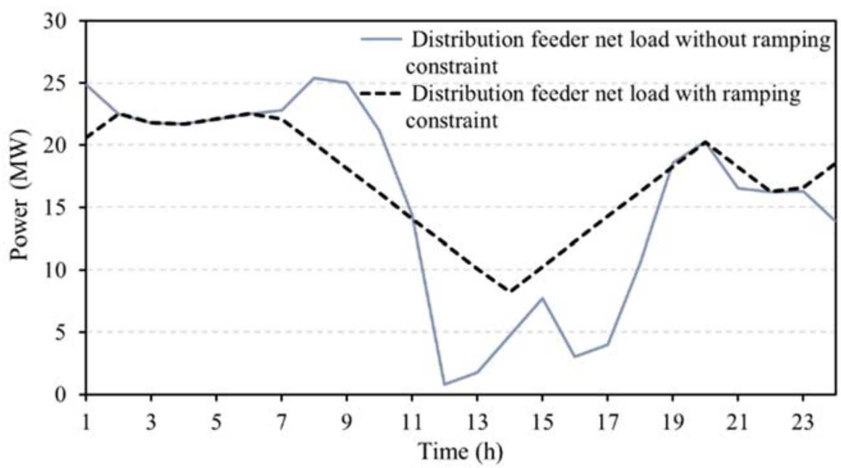

Fig. 4.2 Distribution feeder net load, with and without ramping constraint, for uncertain distributed load over the 24-hour scheduling horizon.

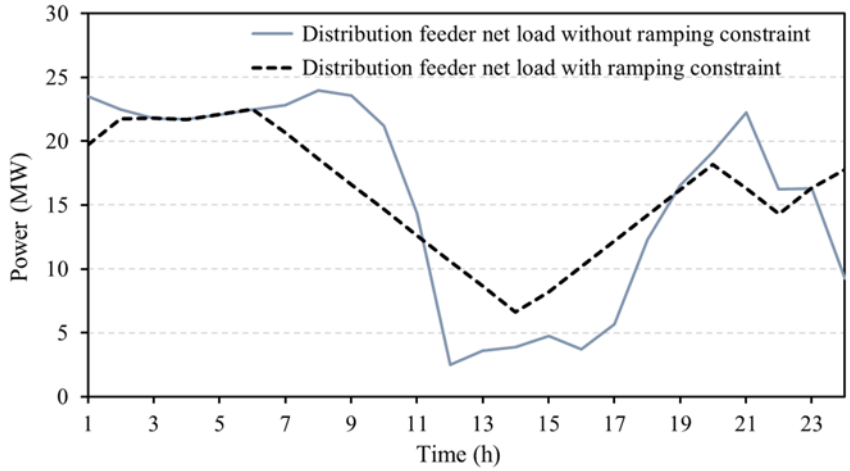

Fig. 4.3 Distribution feeder net load, with and without ramping constraint, for uncertain market price over the 24-hour scheduling horizon.

The obtained results for ±20% solar generation forecast error are almost the same as ±10% load forecast error with minor differences. For ±20% solar generation uncertainty, without any contribution from the microgrid, the utility grid encounters an average of 7.9 MW/h net load change in 3 hours between hours 10 and 12 (with a maximum of 15.75 MW/h), as well as an average of 6.8 MW/h in 2 hours between hours 18 and 19 (a maximum of 7.6 MW/h). The microgrid operation cost when capturing these ramps increases from $11,262.8 to $12,642.2. The results show that although the load forecast error is ±10% compared with ±20% solar generation forecast error, the microgrid operation cost due to contribution in capturing ramping, for load uncertainty has been increased 2.5% more than solar generation uncertainty.

Fig. 4.3 demonstrates the distribution feeder net load with and without considering flexibility constraint for ±10% market price uncertainty. This figure shows the effectiveness of microgrid to address the distribution feeder net load. An average of 7 MW/h ramping in 3 hours in the morning, 11.85 MW/h load change between hours 11 and

12, and 6 MW ramping in one hour between hours 21 and 22 have been mitigated by the microgrid. The obtained results show that the microgrid operation cost is increased by \$1,516.7, equal to 13.3%, due to the addition of the flexibility constraint. It should be noted that in all cases unit 1 is ON for the entire scheduling horizon, while there are changes in commitment and dispatch of other units.

Table 4.3 summarizes the microgrid operation cost for studied cases. It clearly shows that considering uncertainty increases the microgrid operation cost, however it would be able to capture any possible deviations from the forecasted values. The table moreover shows the impact of different uncertainties on the microgrid operation cost.

Table 4.3 Microgrid Operation Cost (\$) for Various Operation Scheduling and 2 MW/h Ramping Limits

Microgrid optimal scheduling	Distributed load uncertainty	Distributed solar uncertainty	Market prices uncertainty
Ignoring uncertainty	\$12126.3	\$12126.3	\$12126.3
Considering uncertainty	\$12915.7	\$12642.1	\$12862.9

Case 3: In this case the microgrid operation cost for various amounts of uncertainty budget are calculated. The obtained results in Table 4.4 illustrate that the microgrid operation cost is directly proportional to the budget of uncertainty. The results further demonstrate that the changes on the load and solar generation have the highest and lowest impact on the microgrid operation cost, respectively. With increasing the budget of uncertainty 0 to 12 hours, the microgrid operation cost is increased by 6.5%, 4.25%, and 6% for distributed load, distributed solar generation, and market price uncertainty, respectively. It should be noted that ±10% was considered for load forecast error and market price uncertainty, whereas ±20% was considered for solar generation uncertainty.

Table 4.4 Microgrid Operation Cost for Various Budgets of Uncertainty (Considering a 2 MW/h Ramping Limit)

Budget of Uncertainty (h)	Distributed load uncertainty	Distributed solar uncertainty	Market price uncertainty
0	$12,126.3	$12,126.3	$12,126.3
3	$12,526.6	$12,393.4	$12,446.1
6	$12,715.3	$12,561.9	$12,611.7
9	$12,850.1	$12,607.9	$12,748.6
12	$12,915.7	$12,642.2	$12,862.9

4.3 Discussions

A flexibility-oriented microgrid optimal scheduling under uncertainty was proposed in this chapter. The robust optimization method was used for capturing uncertainties and increasing the practicality of the proposed model for supporting the utility grid.

- The obtained results showed that utilizing the microgrid decreases the utility ramping to the desired amounts.
- Although flexibility constraints led to higher microgrid operation cost, which should be paid to the microgrid by the electric utility, it removed the need for costly investments on reinforcing the existing electricity infrastructure.
- The numerical simulations further showed that by increasing the budget of uncertainty, the microgrid operation cost increases as it was required to capture uncertainty in a larger number of hours.
- The obtained results indicated that the microgrid operation cost is more sensitive to load uncertainty compared to renewable generation and price uncertainty.

5. Chapter Five: Microgrids Value of Ramping

By leveraging potential flexibility of existing microgrids, viable schemes for addressing the challenging issue of renewable generation integration and supporting distribution grid flexibility were proposed and investigated in previous chapters. However, lacking is the proper valuation mechanism that determines the microgrid value of ramping and enables participation in a distribution market or utility support programs. This chapter builds on the existing work on microgrid ramping but focuses on identifying the true value of the offered ramp. As proposed and modeled in this study, the microgrid operator carries out a cost-benefit analysis to determine the value of ramping to the utility grid. This value, as will be shown in this chapter, will depend on several factors, from the mix of resources that the microgrid utilizes to the number of hours that the microgrid offers ramping services to the grid.

5.1 Model Outline and Problem Formulation

In order to find the microgrid value of ramping, two problems are defined, which are explained in this section. Fig. 5.1 illustrates the flowchart of the proposed model. The first problem is a price-based optimal scheduling which determines the optimal schedule of all DERs and loads as well as exchanged power with the utility grid to ensure a least-cost operation. The second problem is a ramping-oriented optimal scheduling in which an additional constraint is added to the price-based model to account for the required reserved ramping in the microgrid. In this problem, the microgrid controller manages available DERs and loads in a way that not only to supply local loads with least operation cost, but also maintains a specific amount of ramping as reserve (i.e., synchronized with the grid and available to be dispatched) for supporting the utility grid. Accordingly, the microgrid value of ramping is calculated through a comparison of the results of these two problems.

A one-year scheduling horizon is considered for the proposed optimal scheduling models. This extended scheduling horizon would provide adequate amount of data to decide on the value of ramping while at the same time consider variations in loads, generations, and prices through various days, months, and seasons.

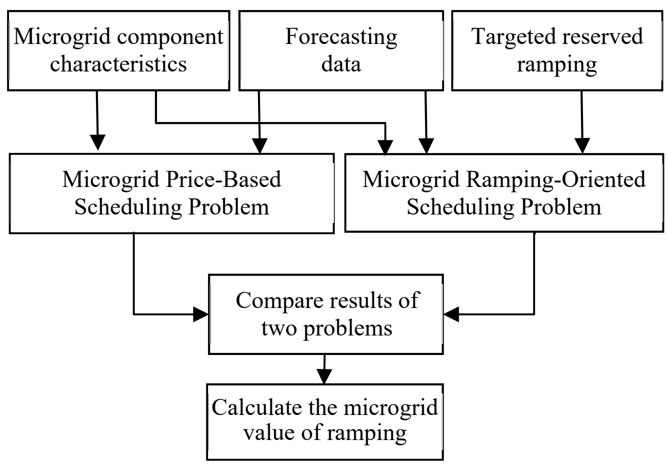

Fig. 5.1 Flowchart of the proposed model for calculation of microgrid value of ramping.

5.1.1 Price-based Ramping-Oriented Optimal Scheduling

In the price-based optimal scheduling, the microgrid is seeking a minimum operation cost as formulated in the following:

$$\min \sum_{h} \sum_{t} [\sum_{i \in G} F_i(P_{iht}) + \rho_{ht}^M P_{ht}^M], \tag{5.1}$$

subject to relevant constraints of microgrid operation which presented in Chapter 4 as equations (4.4)-(4.20).

The first term in the objective function (5.1) is operation cost of dispatchable units and the second term is the revenue or expense of microgrid through power exchange with the utility grid. When the microgrid is purchasing energy from the utility grid, P^M is positive, and when the microgrid is selling its excess energy to the utility grid, P^M is negative, respectively representing a cost and a benefit for the microgrid.

In the ramping-oriented microgrid optimal scheduling, the microgrid not only is responsible for supplying its local loads, but also provides the required ramping to the utility grid. The proposed model is formulated as following:

$$\min \sum_{h}\sum_{t}[\sum_{i\in G} F_i(P_{iht}) + \rho_{ht}^M P_{ht}^M] - \mu \sum_{h}\sum_{t} R_{ht}\,, \tag{5.2}$$

subject to microgrid operation constraints which presented in Chapter 4 as equations (4.4)-(4.20), and

$$\sum_{i\in G} P_i^{\max} I_{iht} + \sum_{i\in\{S,W\}} P_i + P_{ht}^M \geq \sum_{d} D_{dht} + R_{ht} \qquad \forall h, \forall t. \tag{5.3}$$

The objective function is similar to what is used in the price-based optimal scheduling model, however it has an additional term that represents the ramping cost. In the ramping cost, R is the amount of ramping that the microgrid can offer (i.e., reserved power) and μ is the microgrid value of ramping ($/MWh). In order to consider the reserved power in the microgrid to support distribution network flexibility, (5.3) is developed and added to this problem. In this constraint, the summation of the maximum capacity of dispatchable DG of committed units, power generation of non-dispatchable units, and exchanged power with the utility grid should be greater than sum of microgrid loads (fixed and adjustable) and reserved power at each hour. So, (5.3) ensures that the total power generation of local microgrid DERs and exchanged power with the utility grid not only supplies microgrid local demand, but also at least extra power (*R*) is reserved at the desired time intervals in order to support distribution network flexibility. The reserved power (*R*) is considered a time-dependent parameter in the model which gives the ability of considering the reserved ramping capability in any desired time interval, or a series of time intervals, within the scheduling horizon.

5.1.2 Microgrid Value of Ramping Calculations

To find the microgrid value of ramping, the two abovementioned problems are solved and the solutions are compared to find value of ramping. The difference between microgrid operation cost in these two problems is the extra cost which is imposed to the microgrid, owing to considering *R* (MW) reserved ramping to support the utility grid. Therefore, at least the amount of μR, aggregated over all time intervals in the scheduling horizon, should be paid to the microgrid for maintaining unused capacity to offer requested ramping by the utility grid. In other words, the minimum value of ramping is determined as in (5.4):

$$\mu^{\min} = (C^{RO} - C^{PB}) / \sum_{h}\sum_{t} R_{ht} \ , \tag{5.4}$$

where C^{RO} represents the objective value of ramping-oriented microgrid optimal scheduling problem and C^{PB} represents the objective value of price-based microgrid optimal scheduling problem.

5.2 Numerical Simulations

A microgrid with four dispatchable units, two nondispatchable units (wind and solar), one energy storage, and five adjustable loads is utilized for studying the performance of the proposed model. The details of microgrid DERs are borrowed from [83], and annual data for hourly market price, load, wind and solar generation are borrowed from [95]. A maximum ramping capability of 18 MW/h is available in the microgrid, based on the maximum ramping capacity of dispatchable DGs. In addition, a limit of 10 MW is considered as the maximum capacity of the line connecting the microgrid to the utility grid. The developed mixed-integer programming problems are solved using CPLEX 12.6, with a computation time between 5 and 6 minutes for each studied case. The following five cases are investigated:

Case 1: Price-based optimal scheduling

Case 2: Price-based optimal scheduling, considering a 2 MW reserved ramping capability in all operation hours.

Case 3: Price-based optimal scheduling, considering a 2 MW reserved ramping capability in all operation hours, along with uncertainty on load and nondispatchable generation.

Case 4: Price-based optimal scheduling, considering a 2 MW reserved ramping capability in specific operation hours, along with uncertainty on load and nondispatchable generation.

Case 5: Sensitivity analysis of value of ramping with respect to the amount of reserved ramping capability.

Case 1: The grid-connected price-based optimal scheduling problem is solved for the considered one-year horizon as a base case. In this case, the microgrid is only responsible for minimizing its operation cost via managing its dispatchable generation units and adjustable load, and does not have any commitment to the utility grid in terms of ramping. The microgrid operation cost in this case is calculated as $1,720,193.

Case 2: In this case, the microgrid not only is responsible for minimizing its operation cost, but also commits 2 MW as the ramping for supporting the utility grid in all operation hours in the scheduling horizon. Fig. 5.2 depicts the microgrid exchanged power with the utility grid in Cases 1 and 2 in a sample day of the studied year. To realize the microgrid behavior in power arbitrage in various hours of a day, the market price is also shown in this figure.

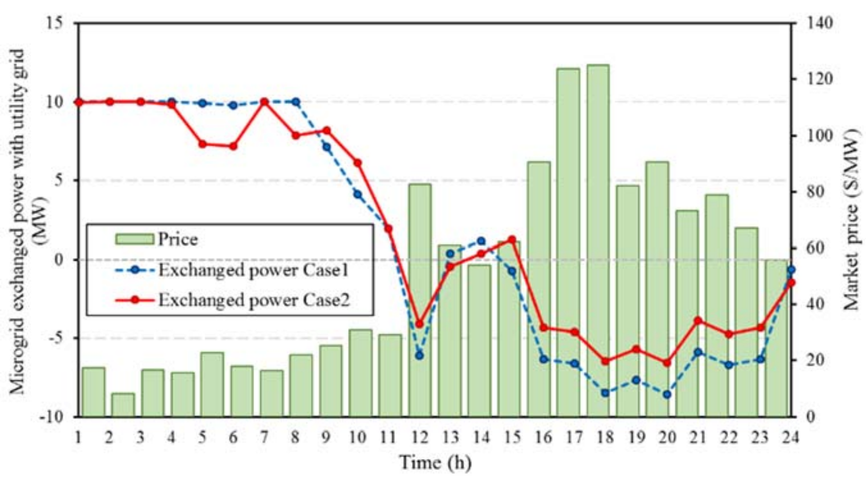

Fig. 5.2 Microgrid exchanged power with the utility grid in a sample day of the studied year, in Case 1 and Case 2.

As this figure shows, in Case 1 the microgrid buys power from the utility grid in full capacity from midnight to early morning, when the market price is the lowest. Then, in the morning, with increasing the market price, microgrid reduces its import power from the utility grid and even at noon it sells excess power back to the utility grid. Again, from early evening to midnight (hours 15 to 24), when the market price is high, microgrid sells its excess power to the utility grid in order to increase its revenue. Thus, in price-based optimal scheduling, microgrid maximizes its revenue via managing its local resources and power exchange with the utility grid. The general trend of microgrid power arbitrage with the utility grid in Case 2 is almost the same as Case 1, since in this case still microgrid aims at minimizing its operation cost. But in addition to minimizing its operation cost, 2 MW is considered as reserved power which means that microgrid has the capability of offering up to 2 MW/h ramping to the utility grid in all hours during the scheduling horizon. The microgrid operation cost in Case 2 increases to \$1,901,963 (10.5% increase compared with Case 1), in expense of offering the ramping service to the utility grid. Furthermore, the microgrid optimal schedule is changed as microgrid sells less power in the afternoon and evening hours, which means a smaller revenue for the microgrid. The difference of microgrid operation cost in these two cases can be used to find the value of ramping, as in (29), which in this case is calculated as \$10.4/MWh. This is the minimum price that should be offered to the microgrid in order to maintain 2 MW reserve ramping in all operation hours within a one-year scheduling horizon.

Case 3: In this case, in addition to considering 2 MW reserved power in all operation hours, +10% and -20% forecast error in load and nondispatchable generation are respectively considered. Since the forecast error in load, solar, and wind generation is inevitable, considering these uncertainties make a more practical case. Furthermore, considering +10% uncertainty for load and -20% for solar/wind generation is the worst-case scenario for the model to be sure that the microgrid will have the capability of offering 2 MW ramping, even if its solar and wind generation drop by 20% and/or the load increases by 10%. The microgrid operation cost in this case increases to \$2,397,799, which is 39% more than Case 1 due to considering 2 MW reserved power along with uncertainty, and 26% more than Case 2 owing to adding aforementioned uncertainties. As the microgrid operation cost in the base case (price-based optimal scheduling) while considering uncertainty is \$2,224,390, the value of ramping for the microgrid in this case is equal to \$9.89/MWh. Fig. 5.3 compares microgrid exchanged power with the utility grid in Cases 2 and 3. As the figure illustrates, considering uncertainty leads to changes in microgrid optimal schedluling. Since the generation of nondispatchable units have been decreased and the local load of microgrid has been increased, in order to still keep 2 MW reserved power, the microgrid buys more power and sells less in all operation hours.

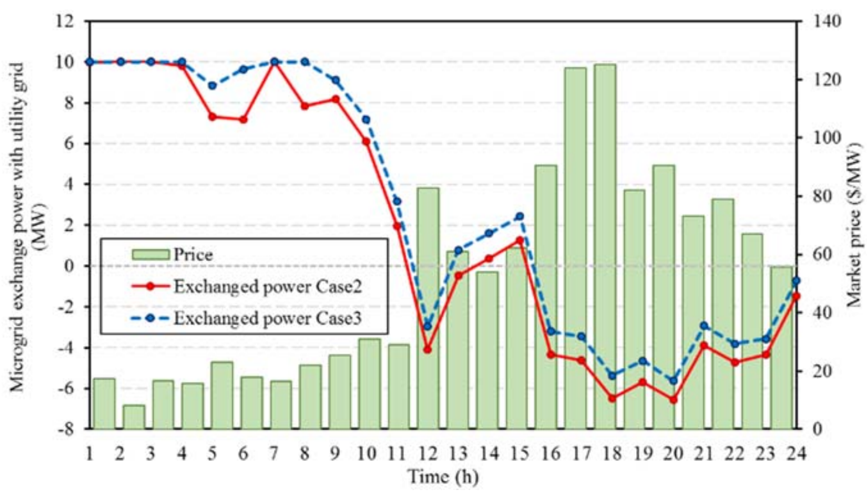

Fig. 5.3 Microgrid exchanged power with the utility grid in a sample day of the studied year, in Case 2 and Case 3.

Case 4: In this case, instead of considering reserved power in all operation hours of a year, it is only considered for the specific hours, specifically at times that the utility grid demand for ramping might be higher. To this end, three hours in 30 different days of a year (mainly peak load hours) are selected for considering a 2 MW reserved power. The microgrid operation cost in this case is \$2,230,500 which is \$6,110 more than microgrid operation cost without consideration of reserved power. Hence, the value of ramping is calculated as \$33.9/MWh.

Case 5: In this case, the sensitivity of microgrid value of ramping with respect to the amount of reserved ramping is analyzed. Fig. 5.4 depicts the microgrid value of ramping for various amounts of reserved power (MW) in two different scenarios: (i) considering reserved ramping for all hours of the year, (ii) considering reserved ramping for only 90 hours of the year.

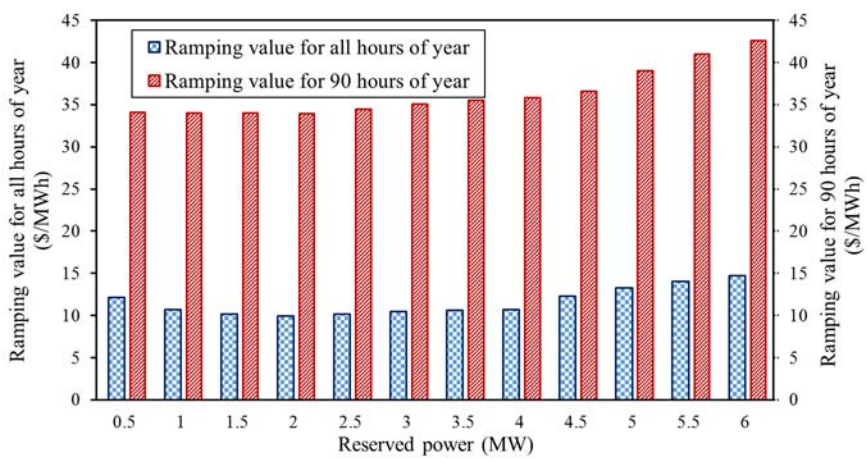

Fig. 5.4 Microgrid ramping value for various amount of reserved ramping capacity and considering uncertainty.

As the figure shows, by increasing the amount of reserved power, the value of ramping slightly decreases (for less than 1 MW for each step) and after that it increases in both scenarios. In addition, the results show the microgrid value of ramping for the lower number of the hours in a year is higher. Because offering ramping services to the utility grid for lower number of hours leads to less total revenue for the microgrid, so the higher value of ramping will compensate the smaller number of hours to make reasonable total revenue for microgrid in order to participate in a distribution market or utility support programs.

Table 5.1 Microgrid Operation Cost ($)

Reserved ramping capacity (MW)	Without Uncertainty		With Uncertainty	
	Reserved ramping for all year	Reserved ramping for 90 hours	Reserved ramping for all year	Reserved ramping for 90 hours
0.0	1,720,193	1,720,193	2,224,390	2,224,390
0.5	1,782,740	1,721,723	2,277,466	2,225,923
1.0	1,822,735	1,723,249	2,317,815	2,227,449
1.5	1,862,287	1,724,775	2,357,755	2,228,975
2.0	1,901,963	1,726,301	2,397,799	2,230,500
2.5	1,950,841	1,727,950	2,446,816	2,232,150
3.0	2,002,903	1,729,666	2,498,886	2,233,866
3.5	2,052,490	1,731,383	2,549,218	2,235,583
4.0	2,101,422	1,733,099	2,599,055	2,237,299
4.5	2,218,898	1,735,017	2,709,186	2,239,217
5.0	2,313,720	1,737,742	2,805,030	2,241,942

Moreover, the microgrid operation cost in various cases, including reserved ramping for all hours and 90 hours of the year, with and without uncertainty, are tabulated in Table I. The obtained results in Table I demonestrate that the microgrid operation cost increases by augmenting reserved ramping capacity, in all cases. In addition, the results prove the significant effect of considering uncertainty on microgrid operation cost. In both conditions of considering reserved power for all hours and 90 hours of the year, uncertainty imposes between 20% and 30% increase on the microgrid operation cost, depending on the amount of considered reserved power. It is worth mentioning that the zero value for reserved power in the table represents the price-based optimal scheduling of the microgrid, i.e. base case.

5.3 Discussions

In this chapter the microgrid value of ramping was calculated through comparing the results of microgrid optimal scheduling and microgrid ramping-oriented scheduling problems. The obtained value of ramping could be a decisive factor for microgrid operator to whether participate in supporting distribution network flexibility or not. Numerical simulations were performed for various situations, considering reserved ramping for all hours and just specific hours of a year as well as different amounts of reserved ramping, to advocate the merits and effectiveness of the proposed model. In addition, the uncertainty on the load and renewable generation were considered in the simulations, as a worst-case. The results demonstrate that the microgrid can calculate its value of ramping, in different situations via the proposed model, in order to have an accurate and reasonable bid for participating in the distribution market or directly supporting the utility grid.

6. Chapter Six: Distribution Market as a Ramping Aggregator for Grid Flexibility Support

Due to significant increase in microgrids deployments in recent years, it is anticipated that, sooner or later, a network of interconnected microgrids will be appearing in power systems [59], [96]–[98]. As a result, microgrids can further be utilized for providing flexibility services in distribution network [99]–[102]. The conclusions drawn from these research efforts advocate that power system operators can considerably take advantage of microgrids to provide flexibility in distribution networks to address the flexibility-associated bottlenecks.

The rapid deployment of microgrids, as well as other proactive customers in distribution networks, has made the case for extending the concept of a Distribution System Operator (DSO) to manage the interaction of these customers with the upstream network as well as with the wholesale market [103]. The existing literature in this research area lacks studies on the microgrids participation on distribution ramping market. Along with the current trend in proposing electricity markets in distribution networks [103], this study deals with the distribution ramping support under the concept of a Distribution Market Operator (DMO), which is the equivalent of an ISO but in the distribution level [104].

6.1 Model Outline and Problem Formulation

Microgrids have been already proposed as a flexibility resource for increasing the flexibility of the power system and supporting the utility grid to capture the utility ramping, variabilities, and uncertainties. In line with demand bidding, microgrids can submit their ramping capability to the DMO at each hour. Fig. 6.1 shows the schematic diagram which demonstrates the interactions of different involved players including the ISO, the DMO and microgrids in the market [105].

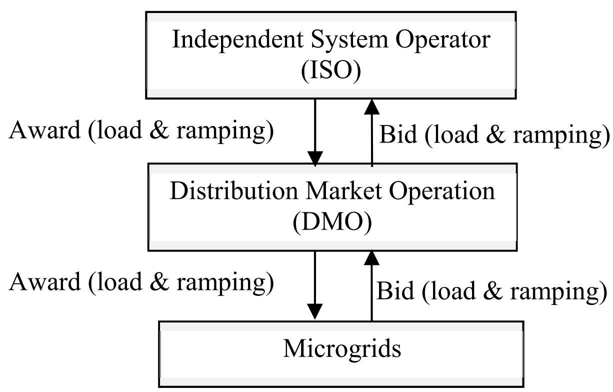

Fig. 6.1 Participation of microgrids in ramping market through the DMO.

As illustrated in the above schematic diagram, the DMO is responsible for two tasks; aggregating microgrids ramping and demand bids and disaggregating the awards from the ISO. In the first step, the DMO combines individual ramping and demand bids received from microgrids, aggregates them, and submits the aggregated bid to the ISO in order to participate in the wholesale energy market. In the second step, the DMO disaggregates the awarded quantity, for both demand and ramping, received from the ISO to microgrids, based on their initially submitted bids. Fig. 6.2 provides an illustrative example of aggregating ramping curves by the DMO [105].

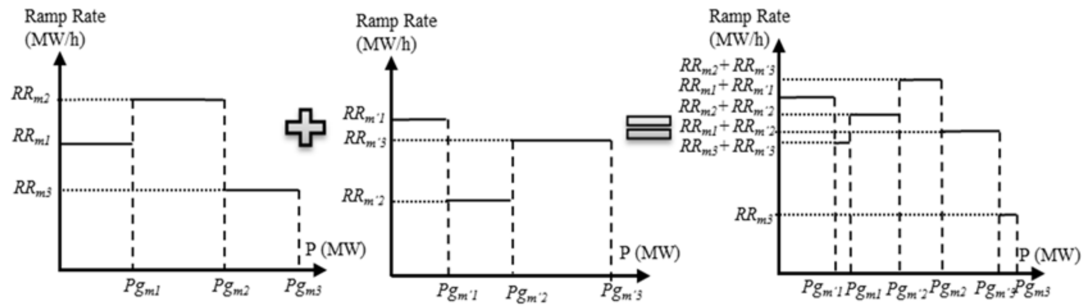

Fig. 6.2 An example of DMO aggregation; two submitted ramping bids by microgrids *m* and *m'* are aggregated in the DMO.

Fig. 6.3 demonstrates a typical demand bid curve submitted by mth microgrid to the DMO at a sample hour *t*. The fixed part of the loads d^f is not curtailable or shiftable and should be supplied by the utility grid under any circumstances, while the variable part of the bid represents the microgrid flexibility in altering its consumption through load adjustment (which can be done by load curtailment, load shifting, or local generation increase). The summation of all microgrids' fixed loads provides the total fixed load which should be supplied by the DMO (6.1).

$$D_t^f = \sum_m d_{mt}^f \qquad \forall m, \forall t, \tag{6.1}$$

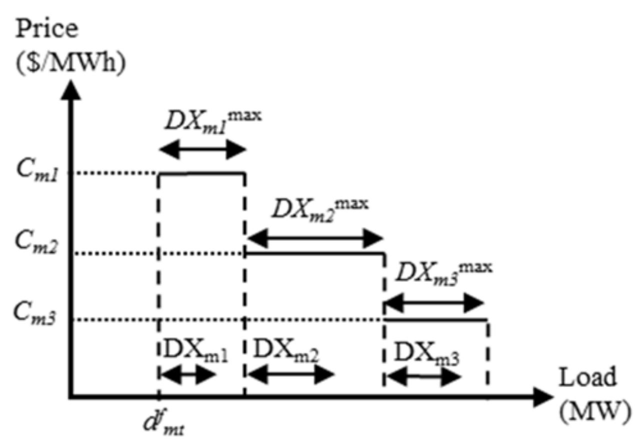

Fig. 6.3 A typical demand bid curve for microgrid *m*.

After assigning power to the DMO by the ISO, the DMO disaggregates the awarded power to the microgrids. The DMO is aimed at maximizing the demand benefit as in (6.2) by assigning the optimal awarded power to each microgrid, in accordance with their respective submitted ramping and demand bids.

$$\max \sum_t \sum_m \sum_g c_{mg} DX_{mgt} \tag{6.2}$$

$$\varepsilon\, \delta_{mgt} \le DX_{mgt} \le DX_{mg}^{\max} \delta_{mgt} \qquad \forall m, \forall t, \forall g, \tag{6.3}$$

$$\delta_{mgt} \le \delta_{m(g-1)t} \qquad \forall m, \forall t, \forall g, \tag{6.4}$$

$$d_{mt}^{r} = \sum_g DX_{mgt} \qquad \forall m, \forall t, \tag{6.5}$$

$$d_{mt}^{r} + d_{mt}^{f} = PD_{mt}^{M} \qquad \forall m, \forall t, \tag{6.6}$$

$$\sum_m PD_{mt}^{M} = D_{bt} \qquad \forall t. \tag{6.7}$$

Each load segment is bounded by (6.3), where binary status variable δ determines which segments are selected in the optimization model (δ_g is one when segment g has the value of DX_g, and it is zero when segment g is not selected). Constraint (6.4) ensures that the segments are selected in a sequential order. The total responsive load of each microgrid equals to the summation of the loads dispatched to each segment (6.5). The summation of fixed and responsive loads equals to the awarded load to microgrids by the DMO (6.6). The total demand awarded from the ISO to the DMO is further equal to the summation of the awarded load to microgrids by the DMO (6.7). Constraints (6.8) and (6.9) are considered in the model to satisfy the desired utility grid ramping at each hour (Δ_t). This desired ramping is supplied by all the participated microgrids in the DSO market. The specific amount of ramping is assigned to each microgrid based on their respective ramping bid.

$$RR_t^{Total} = \sum_m RR_{mt}^{Sel} \qquad \forall t, \tag{6.8}$$

$$RR_t^{Total} > \Delta_t \qquad \forall t, \tag{6.9}$$

$$-M(1-\delta_{mgt} + \sum_{k>g} \delta_{mkt}) \le RR_{mt}^{Sel} - RR_{mg} \le M(1-\delta_{mgt} + \sum_{k>g} \delta_{mkt}) \qquad \forall m, \forall g, \forall t, \tag{6.10}$$

$$-M \sum_k \delta_{mkt} \le RR_{mg} \le M \sum_k \delta_{mkt} \qquad \forall m, \forall g, \forall t. \tag{6.11}$$

In order to pair the selected segments of the awarded load with the corresponding ramping capability of those segments, (6.10) is developed. This constraint is employed for ramping and demand bid curve with N_g segments, which ensures that by selecting any of the segments of the awarded load, the corresponding ramping value will be selected. On the other hand, if none of the segments are selected, the ramping value will become zero (6.11) [105].

6.2 Numerical Examples

In this section, the proposed model is applied to a test system. A total of 5 microgrids with the total installed DG capacity of 69 MW are considered. Each microgrid consists of 4 dispatchable units with the specifications listed in Table 6.1. Fixed load of each microgrid as well as the total demand awarded to all microgrids from the DMO are plotted in Fig. 6.4 for 24 hours. It should be noted that as this paper focuses on the role of the DMO and the participated microgrids in the market, a predefined and fixed value is considered as the total demand awarded from the ISO to the DMO.

The developed mixed-integer programming problem is solved using CPLEX 12.6. The following cases are studied [105]:

Case 1: Market-based microgrid scheduling.

Case 2: Market-based microgrid scheduling considering ramping constraints.

Table 6.1 Marginal Costs ($/MWh), Capacity (MW) and Ramp Rate (MW/h)

	Price ($/MWh)				
	MG1	MG2	MG3	MG4	MG5
DG1	71.5	62.8	64.5	69.5	76.5
DG2	58.4	50.5	59.8	57.2	62.4
DG3	45.2	33.6	46.2	38.4	40.5
DG4	23.2	25.7	27.4	27.9	31.1
	Capacity (MW)				
DG1	5	4	5	5	5
DG2	5	4	3	5	4
DG3	3	2	3	4	3
DG4	2	2	1	2	2
	Ramping rate (MW/h)				
DG1	3	2.5	3.5	2	3
DG2	2	2	1.5	2	1
DG3	3	2	1.5	3	2
DG4	1.5	1	0.5	1	1

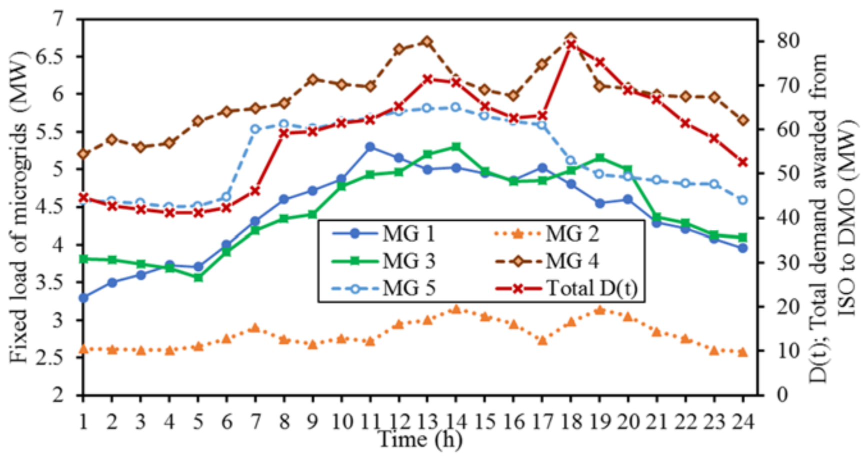

Fig. 6.4 Fixed load of microgrids and total awarded demand from the ISO to the DMO (MW).

Case 1: In this case, the load awarded from the ISO to the DMO is distributed between the microgrids based on their bids, while the objective function (6.2) is maximized. In this case, the DMO does not have any responsibility for providing the ramping to the ISO. The value of awarded load to the microgrids in this case equals $56,286.

Case 2: In this case, a total ramping of 12.5 MW/h is considered as the desired ramping value that the DMO is expected to provide to the ISO. The DMO market scheduling problem is solved again with this new constraint. Fig. 6.5 compares the total ramping capability of all microgrids in Cases 1 and 2. As this figure shows, in Case 2, the participated microgrids provide to at least 12.5 MW/h ramping capability for all hours of the scheduling horizon, which the DMO can reliably deliver to the ISO upon request. This guaranteed ramping should be compared with the available ramping in Case 1, in which is variable, necessarily not guaranteed, and can significantly drop based on microgrids operation.

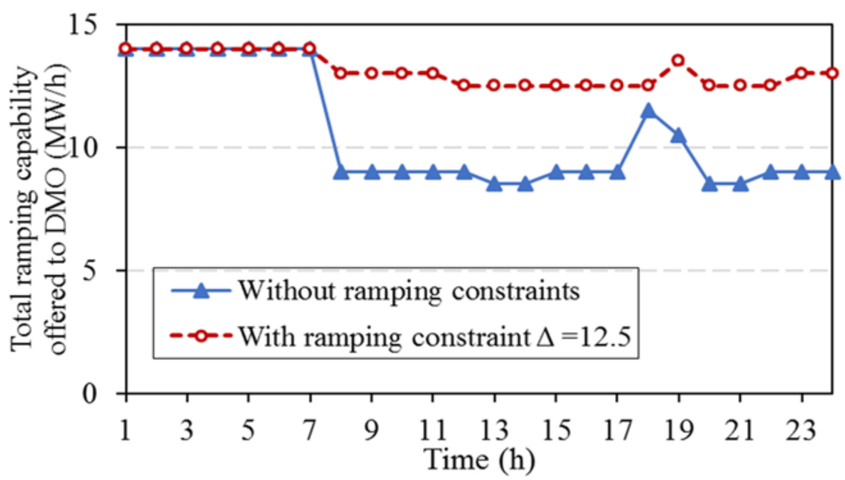

Fig. 6.5 Total ramping capability of all microgrids offered to the DMO (MW/h).

Fig. 6.5 compares the awarded load to all 5 microgrids in Cases 1 and 2. Figs 6.6(a)-6.6(e) clearly demonstrate how the distribution of the awarded load among the microgrids is alterd based on their ramping and demand bid to the DMO for achieving a 12.5 MW/h ramping capability. For instance, in microgrid 1, Fig 6.6(a), the awarded load at hours 13, 14, 20, and 21 increases from 10 MW, which leads to moving to the next ramping curve segment with a higher ramping capability (moving from ramp rate of 2 MW/h to 3 MW/h). In Fig. 6.6 (c) the awarded load to the microgrid 3 decreases in all 24 hours to the first segment (5 MW) which has a larger ramp rate, i.e. 3.5 MW/h. The distribution of the awarded load among the different dispatchable units of microgrids 2, 4 and 5 (Figs 6.6(b), 6.6(d), 6.6(e)) is changed in the same manner to achieve the desired ramping capability. It is intersting to note that the objective value in Case 2 is calcualted as \$55,751 (\$535 less than Case 1), which is considerably small compared to the significant benefit that the DMO can provide to the ISO.

It is worthwhile to mention that the total awarded load (summation of fixed and adjustable loads) to all microgrids in both cases is exactly the same. However, as Fig. 6.6 depicts, it is distributed differently among microgrids in order to meet the ramping constraint.

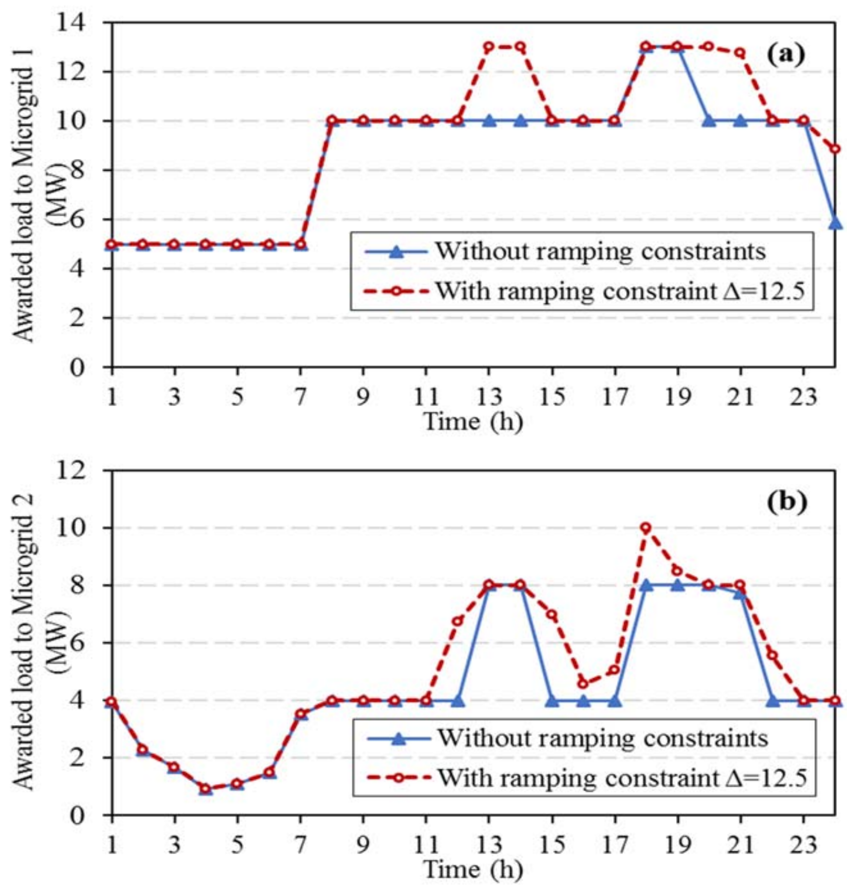

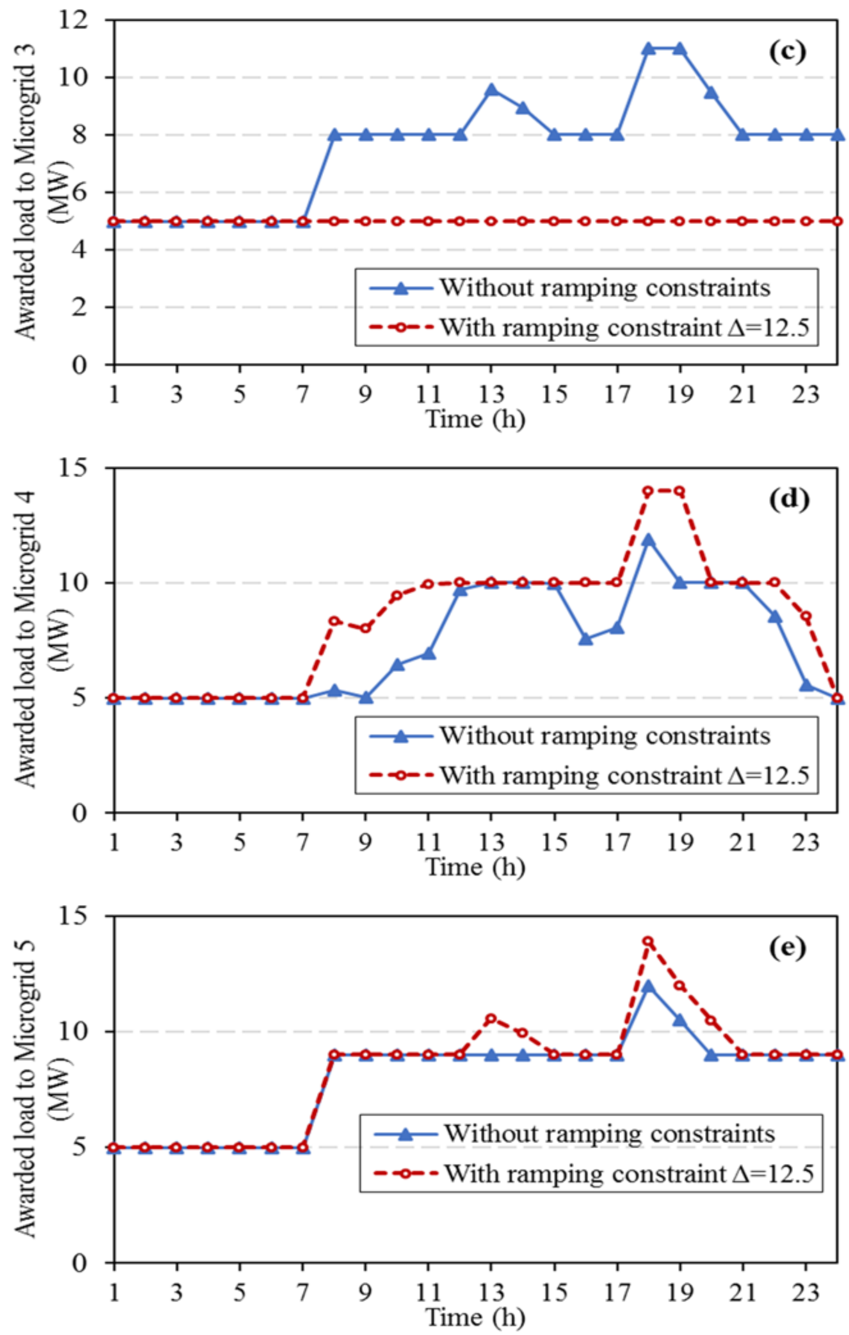

Fig. 6.6 Comparison of load awarded to all microgrids in two cases with and without ramping constraints.

Table 6.2 demonestrates the DG commitments in each microgrid in Case 2, where the highlithed cells represent the changes from Case 1. As the table shows, some of the DG commitments are changed in order to provide the desired ramping to the DMO and consequently to the ISO.

Table 6.2 The Unit Commitment Schedule of Microgrids

		Time (h)																							
		1	**2**	**3**	**4**	**5**	**6**	**7**	**8**	**9**	**10**	**11**	**12**	**13**	**14**	**15**	**16**	**17**	**18**	**19**	**20**	**21**	**22**	**23**	**24**
MG 1	**DG 1**	1	1	1	1	1	1	1	1	1	1	1	1	1	1	1	1	1	1	1	1	1	1	1	1
	DG 2	0	0	0	0	0	0	0	1	1	1	1	1	1	1	1	1	1	1	1	1	1	1	1	1
	DG 3	0	0	0	0	0	0	0	0	0	0	0	0	**1**	**1**	0	0	0	1	1	**1**	**1**	0	0	0
	DG 4	0	0	0	0	0	0	0	0	0	0	0	0	0	0	0	0	0	0	0	0	0	0	0	0
MG 2	**DG 1**	1	1	1	1	1	1	1	1	1	1	1	1	1	1	1	1	1	1	1	1	1	1	1	1
	DG 2	0	0	0	0	0	0	0	0	0	0	0	**1**	1	1	**1**	**1**	**1**	1	1	1	1	**1**	0	0
	DG 3	0	0	0	0	0	0	0	0	0	0	0	0	0	0	0	0	0	**1**	**1**	0	0	0	0	0
	DG 4	0	0	0	0	0	0	0	0	0	0	0	0	0	0	0	0	0	0	0	0	0	0	0	0
MG 3	**DG 1**	1	1	1	1	1	1	1	1	1	1	1	1	1	1	1	1	1	1	1	1	1	1	1	1
	DG 2	0	0	0	0	0	0	0	**0**	**0**	**0**	**0**	**0**	**0**	**0**	**0**	**0**	**0**	**0**	**0**	**0**	**0**	**0**	**0**	**0**
	DG 3	0	0	0	0	0	0	0	0	0	0	0	0	**0**	**0**	0	0	0	**0**	**0**	**0**	0	0	0	0
	DG 4	0	0	0	0	0	0	0	0	0	0	0	0	0	0	0	0	0	0	0	0	0	0	0	0
MG 4	**DG 1**	1	1	1	1	1	1	1	1	1	1	1	1	1	1	1	1	1	1	1	1	1	1	1	1
	DG 2	0	0	0	0	0	0	0	1	**1**	1	1	1	1	1	1	1	1	1	1	1	1	1	1	0
	DG 3	0	0	0	0	0	0	0	0	0	0	0	0	0	0	0	0	0	1	**1**	0	0	0	0	0
	DG 4	0	0	0	0	0	0	0	0	0	0	0	0	0	0	0	0	0	0	0	0	0	0	0	0
MG 5	**DG 1**	1	1	1	1	1	1	1	1	1	1	1	1	1	1	1	1	1	1	1	1	1	1	1	1
	DG 2	0	0	0	0	0	0	0	1	1	1	1	1	1	1	1	1	1	1	1	1	1	1	1	1
	DG 3	0	0	0	0	0	0	0	0	0	0	0	0	**1**	**1**	0	0	0	1	1	**1**	0	0	0	0
	DG 4	0	0	0	0	0	0	0	0	0	0	0	0	0	0	0	0	0	**1**	0	0	0	0	0	0

6.3 Discussions

A distribution market scheduling model was proposed in this chapter. The proposed scheduling model was developed to capture and collect the ramping capability of participating microgrids in the distribution market as to offer it to the upstream network. Using the proposed model, DMOs can appear as major sources of flexibility in the system to address emerging ramping issues in the system associated with growing proliferation of variable renewable generation. The proposed model was analyzed through numerical simulations, where it was shown that the offered ramping capability could be significant, considering the DMO would collect the ramping capability of a large number of microgrids, and if available, other proactive customers. This offering will be at the expense of minor deviation in microgrids schedules from their optimal operating point, which would require additional discussions on a proper incentive mechanism as follow on work.

7. Chapter Seven: Conclusion and Future Directions

Renewable energy resource deployment has experienced a significant global growth over the last decade, conceivably due to its environmental benefits and the recent drops in the development and deployment cost of the technology. The increase in renewable generation, however, has resulted in new challenges in supply-load balancing, owing to its intermittent, non-predictable and volatile generation features. Application of microgrids in capturing the variabilities of distributed renewable generation in distribution networks is proposed and investigated in this dissertation as a novel method to cope with negative impacts of the renewable generation deployment. Utilizing available flexibility of microgrids represents a local and viable solution which leads to lower investments from electric utilities for increasing their flexibility and providing more reserved power. It was investigated that how the system flexibility requirements can be integrated into the microgrid optimal scheduling model to enable microgrids in supporting the grid operators by offering flexibility services.

In this dissertation, a flexibility-oriented microgrid optimal scheduling model was proposed to efficiently schedule microgrid resources for supporting the distribution grid flexibility requirements. These flexibility requirements were considered in terms of net load ramping limits. The model was studied for intra-hour and inter-hour time intervals during the 24-hour day-ahead operation. In addition, a robust optimization method was used for capturing uncertainties and increasing the practicality of the proposed model for supporting the utility grid.

Furthermore, a flexibility-oriented microgrid optimal scheduling model was proposed in this dissertation to efficiently schedule microgrid resources to support utility grid operation via providing ancillary services. The proposed model considered intra-hour and inter-hour time intervals during the 24-hour day-ahead scheduling horizon, offering 1-minute frequency regulation service, 10-minute load following service, and hourly ramping service.

Moreover, the microgrid value of ramping was calculated in this dissertation which could be a decisive factor for microgrid operator to whether participate in supporting distribution network flexibility or not.

In addition, a distribution market scheduling model was proposed in this study. The proposed scheduling model was developed to capture and collect the ramping capability of participating microgrids in the distribution market as to offer it to the upstream network. Using the proposed model, DMOs can appear as major sources of flexibility in the system to address emerging ramping issues in the system associated with growing proliferation of variable renewable generation.

Considering a network of microgrids for providing flexibility support and other ancillary services to the utility grid could be considered as the next step of this work. In this study, only the active power was considered in the models. Investigation of reactive power and providing reactive power control to the utility grid by microgrids could also be the next step of this work which can give voltage control to the utility grids as another ancillary service option. In addition, cost-benefit analysis is essential for microgrid owners as a decisive factor for participation on supporting the utility grid. This subject was considered in parts of this work but needs further study to obtain an accurate and comprehensive cost-benefit analysis model.

References

[1] Ren21, "The First Decade: 2004-2014, 10 Years of Renewable Energy Progress," pp. 2004–2014, 2014.

[2] REN21, "Renewables 2017: global status report," 2017.

[3] REN21, "Renewables 2018:global status report," 2018.

[4] U.S. EIA, "Annual Energy Review 2011," 2012.

[5] G. Barbose, N. Darghouth, and S. Weaver, "Tracking the Sun VII: An Historical Summary of the Installed Price of Photovoltaics in the United States from 1998 to 2013," Lawrence Berkeley National Laboratory, Sept. 2014.

[6] P. Denholm, M. O'Connell, G. Brinkman, and J. Jorgenson, "Overgeneration from Solar Energy in California. A Field Guide to the Duck Chart," National Renewable Energy Lab.(NREL), Golden, CO, 2015.

[7] "What the duck curve tells us about managing a green grid," *California ISO*. [Online]. Available: https://www.caiso.com/Documents/FlexibleResourcesHelpRenewables_FastFacts.pdf.

[8] California ISO, "Flexible Ramping Products: Revised Draft Final Proposal," pp. 1–18, 2015.

[9] C. Monteiro, R. Bessa, V. Miranda, a. Botterud, J. Wang, and G. Conzelmann, "Wind Power Forecasting: State-of-the-Art 2009 Decision and Information Sciences Division," *Argonne Natl. Lab.*, no. November 6, pp. 1–216, 2009.

[10] S. Pelland, J. Remund, J. Kleissl, T. Oozeki, and K. De Brabandere, “Photovoltaic and solar forecasting: state of the art,” *IEA PVPS, Task*, vol. 14, pp. 1–36, 2013.

[11] L. Hernández, C. Baladrón, J. M. Aguiar, B. Carro, A. Sánchez-Esguevillas, and J. Lloret, “Artificial neural networks for short-term load forecasting in microgrids environment,” *Energy*, vol. 75, pp. 252–264, 2014.

[12] E. B. Ssekulima, M. B. Anwar, A. Al Hinai, and M. S. El Moursi, “Wind speed and solar irradiance forecasting techniques for enhanced renewable energy integration with the grid: a review,” *IET Renew. Power Gener.*, vol. 10, no. 7, pp. 885–989, 2016.

[13] A. Kaur, L. Nonnenmacher, and C. F. M. Coimbra, “Net load forecasting for high renewable energy penetration grids,” *Energy*, vol. 114, pp. 1073–1084, Nov. 2016.

[14] M. Alanazi, M. Mahoor, and A. Khodaei, “Day-Ahead Solar Forecasting Based on Multi-Level Solar Measurements,” *2018 IEEE/PES Transmission and Distribution Conference and Exposition (T&D)*, Denver, CO, 2018, pp. 1–9.

[15] M. Alanazi, M. Mahoor, and A. Khodaei, “Two-stage hybrid day-ahead solar forecasting,” *2017 North American Power Symposium (NAPS)*, Morgantown, WV, 2017, pp. 1–6.

[16] F. Golestaneh, P. Pinson, and H. B. Gooi, “Very Short-Term Nonparametric Probabilistic Forecasting of Renewable Energy Generation— With Application to Solar Energy,” *IEEE Trans. Power Syst.*, vol. 31, no. 5, pp. 3850–3863, 2016.

[17] J. R. Andrade and R. J. Bessa, “Improving Renewable Energy Forecasting With a Grid of Numerical Weather Predictions,” *IEEE Trans. Sustain. Energy*, vol. 8, no.

4, pp. 1571–1580, 2017.

[18] R. Eskandarpour and A. Khodaei, “Machine Learning Based Power Grid Outage Prediction in Response to Extreme Events,” *IEEE Trans. Power Syst.*, vol. 32, no. 4, pp. 3315–3316, 2017.

[19] I. Hiskens and D. Callaway, “Achieving controllability of plug-in electric vehicles,” *5th IEEE Veh. Power Propuls. Conf. VPPC ’09*, pp. 1215–1220, 2009.

[20] M. Beaudin, H. Zareipour, A. Schellenberglabe, and W. Rosehart, “Energy storage for mitigating the variability of renewable electricity sources: An updated review,” *Energy Sustain. Dev.*, vol. 14, no. 4, pp. 302–314, 2010.

[21] B. A. Frew, S. Becker, M. J. Dvorak, G. B. Andresen, and M. Z. Jacobson, “Flexibility mechanisms and pathways to a highly renewable US electricity future,” *Energy*, vol. 101, pp. 65–78, 2016.

[22] M. I. Alizadeh, M. Parsa Moghaddam, N. Amjady, P. Siano, and M. K. Sheikh-El-Eslami, “Flexibility in future power systems with high renewable penetration: A review,” *Renew. Sustain. Energy Rev.*, vol. 57, pp. 1186–1193, May 2016.

[23] A. J. Lamadrid and T. Mount, “Ancillary services in systems with high penetrations of renewable energy sources, the case of ramping,” *Energy Econ.*, vol. 34, no. 6, pp. 1959–1971, 2012.

[24] Y. Dvorkin, D. S. Kirschen, and M. a. Ortega-Vazquez, “Assessing flexibility requirements in power systems,” *IET Gener. Transm. Distrib.*, vol. 8, no. 11, pp. 1820–1830, 2014.

[25] H. Wu, A. Al-Abdulwahab, and M. Shahidehpour, “Hourly demand response in day-

ahead scheduling for managing the variability of renewable energy," *IET Gener. Transm. Distrib.*, vol. 7, no. 3, pp. 226–234, 2013.

[26] N. Navid and G. Rosenwald, "Market solutions for managing ramp flexibility with high penetration of renewable resource," *IEEE Trans. Sustain. Energy*, vol. 3, no. 4, pp. 784–790, 2012.

[27] E. Lannoye, D. Flynn, and M. O'Malley, "Evaluation of power system flexibility," *IEEE Trans. Power Syst.*, vol. 27, no. 2, pp. 922–931, 2012.

[28] H. Nosair and F. Bouffard, "Flexibility Envelopes for Power System Operational Planning," *IEEE Trans. Sustain. Energy*, vol. 6, no. 3, pp. 800–809, 2015.

[29] P. Denholm, E. Ela, B. Kirby, and M. Milligan, "The Role of Energy Storage with Renewable Electricity Generation The Role of Energy Storage with Renewable Electricity Generation," NREL, January 2010.

[30] M. A. Ortega-Vazquez and D. S. Kirschen, "Estimating the spinning reserve requirements in systems with significant wind power generation penetration," *IEEE Trans. Power Syst.*, vol. 24, no. 1, pp. 114–124, 2009.

[31] A. Ulbig and G. Andersson, "On operational Flexibility in Electric Power Systems," *IEEE Power and Energy Society General Meeting*, San Diego, CA, 2012, pp. 1-8.

[32] D. S. Kirschen, A. Rosso, J. Ma, and L. F. Ochoa, "Flexibility from the demand side," *2012 IEEE Power and Energy Society General Meeting*, San Diego, CA, 2012, pp. 1-6.

[33] M. Ghamkhari and H. Mohsenian-Rad, "Optimal integration of renewable energy resources in data centers with behind-the-meter renewable generator," *2012 IEEE*

International Conference on Communications (ICC), Ottawa, ON, 2012, pp. 3340-3344.

[34] A. Asadinejad and K. Tomsovic, “Impact of Incentive Based Demand Response on large scale renewable integration,” *2016 IEEE Power & Energy Society Innovative Smart Grid Technologies Conference (ISGT)*, Minneapolis, MN, 2016, pp. 1-5.

[35] S.-C. Chan, K. M. Tsui, H. C. Wu, Y. Hou, Y.-C. Wu, and F. F. Wu, “Load/price forecasting and managing demand response for smart grids: Methodologies and challenges,” *IEEE Signal Process. Mag.*, vol. 29, no. 5, pp. 68–85, 2012.

[36] O. Ma *et al.*, “Demand Response for Ancillary Services,” *IEEE Trans. Smart Grid*, vol. 4, no. 4, pp. 1988–1995, 2013.

[37] J. Aghaei and M. I. Alizadeh, “Demand response in smart electricity grids equipped with renewable energy sources: A review,” *Renew. Sustain. Energy Rev.*, vol. 18, pp. 64–72, 2013.

[38] S. Mohajeryami, I. N. Moghaddam, M. Doostan, B. Vatani, and P. Schwarz, “A novel economic model for price-based demand response,” *Electr. Power Syst. Res.*, vol. 135, pp. 1–9, 2016.

[39] L. Wang, Z. Wang, and R. Yang, “Intelligent multiagent control system for energy and comfort management in smart and sustainable buildings,” *IEEE Trans. Smart Grid*, vol. 3, no. 2, pp. 605–617, 2012.

[40] N. Zareen, M. W. Mustafa, U. Sultana, R. Nadia, and M. A. Khattak, “Optimal real time cost-benefit based demand response with intermittent resources,” *Energy*, vol. 90, pp. 1695–1706, 2015.

[41] M. Mahoor, N. Iravani, S. M. Salamati, A. Aghabali, and A. Rahimi-Kian, “Smart energy management for a micro-grid with consideration of demand response plans,” *2013 Smart Grid Conference (SGC)*, Tehran, 2013, pp. 125-130.

[42] J. Eyer and G. Corey, “Energy Storage for the Electricity Grid : Benefits and Market Potential Assessment Guide A Study for the DOE Energy Storage Systems Program,” 2010.

[43] P. Denholm and M. Hand, “Grid flexibility and storage required to achieve very high penetration of variable renewable electricity,” *Energy Policy*, vol. 39, no. 3, pp. 1817–1830, 2011.

[44] K. Bradbury, L. Pratson, and D. Patino-Echeverri, “Economic viability of energy storage systems based on price arbitrage potential in real-time U.S. electricity markets,” *Appl. Energy*, vol. 114, pp. 512–519, 2014.

[45] N. Gast, D.-C. Tomozei, and J.-Y. Le Boudec, “Optimal generation and storage scheduling in the presence of renewable forecast uncertainties,” *IEEE Trans. Smart Grid*, vol. 5, no. 3, pp. 1328–1339, 2014.

[46] E. Hajipour, M. Bozorg, and M. Fotuhi-Firuzabad, “Stochastic capacity expansion planning of remote microgrids with wind farms and energy storage,” *IEEE Trans. Sustain. Energy*, vol. 6, no. 2, pp. 491–498, 2015.

[47] L. Barelli, U. Desideri, and A. Ottaviano, “Challenges in load balance due to renewable energy sources penetration: The possible role of energy storage technologies relative to the Italian case,” *Energy*, vol. 93, pp. 393–405, 2015.

[48] S. Gottwalt, A. Schuller, C. Flath, H. Schmeck, and C. Weinhardt, “Assessing load

flexibility in smart grids: Electric vehicles for renewable energy integration,” *2013 IEEE Power & Energy Society General Meeting*, Vancouver, BC, 2013, pp. 1-5.

[49] S. Inage, "Modelling Load Shifting Using Electric Vehicles in a Smart Grid Environment", *IEA Energy Papers*, 2010, No. 2010/07, OECD Publishing, Paris, https://doi.org/10.1787/5km7v0bsmw7k-en.

[50] A. Abiri-Jahromi, A. Majzoobi, A. Khodaei, S. Bahramirad, L. Zhang, A. Paaso, M. Lelic, D. Flinn, "Battery energy storage requirements for mitigating PV output fluctuations," *2018 IEEE PES Innovative Smart Grid Technologies Conference Europe (ISGT-Europe)*, Sarajevo, 2018, pp. 1-5.

[51] E. M. G. Rodrigues, R. Godina, S. F. Santos, A. W. Bizuayehu, J. Contreras, and J. P. S. Catalao, “Energy storage systems supporting increased penetration of renewables in islanded systems,” *Energy*, vol. 75, pp. 265–280, 2014.

[52] H. Lotfi, A. Majzoobi, A. Khodaei, S. Bahramirad, and A. Paaso, “Levelized Cost of Energy Calculation for Energy Storage Systems,” in *CIGRE Grid of the Future Symposium,* Philadelphia, PA, 2016.

[53] H. Kamankesh, V. G. Agelidis, and A. Kavousi-Fard, “Optimal scheduling of renewable micro-grids considering plug-in hybrid electric vehicle charging demand,” *Energy*, vol. 100, pp. 285–297, 2016.

[54] P. M. R. Almeida, J. A. P. Lopes, F. J. Soares, and L. Seca, “Electric vehicles participating in frequency control: Operating islanded systems with large penetration of renewable power sources,” *2011 IEEE PES Trondheim PowerTech Power Technol. a Sustain. Soc. POWERTECH 2011*, vol. 1, pp. 5–10, 2011.

[55] Microgrid Exchange Group, “DOE Microgrid Workshop Report,” 2011. [Online]. Available: http://energy.gov/oe/downloads/microgrid-workshop-report-august-2011.

[56] F. Katiraei, R. Iravani, N. Hatziargyriou, and A. Dimeas, “Microgrids management,” *IEEE Power Energy Mag.*, vol. 6, no. 3, pp. 54–65, 2008.

[57] J. A. P. Lopes, C. L. Moreira, and A. G. Madureira, “Defining control strategies for MicroGrids islanded operation,” *IEEE Trans. Power Syst.*, vol. 21, no. 2, pp. 916–924, 2006.

[58] P. Piagi and R. H. Lasseter, “Autonomous control of microgrids,” *2006 IEEE Power Engineering Society General Meeting*, Montreal, Que., 2006, pp. 1-8.

[59] S. Parhizi, H. Lotfi, A. Khodaei, and S. Bahramirad, “State of the art in research on microgrids: A review,” *IEEE Access*, vol. 3, pp. 890–925, 2015.

[60] A. G. Tsikalakis and N. D. Hatziargyriou, “Centralized control for optimizing microgrids operation,” *2011 IEEE Power and Energy Society General Meeting*, Detroit, MI, USA, 2011, pp. 1-8.

[61] N. W. A. Lidula and A. D. Rajapakse, “Microgrids research: A review of experimental microgrids and test systems,” *Renew. Sustain. Energy Rev.*, vol. 15, no. 1, pp. 186–202, Jan. 2011.

[62] M. Mahoor, A. Majzoobi, and A. Khodaei, “Distribution asset management through coordinated microgrid scheduling,” *IET Smart Grid*, vol. 1, no. 4, pp. 159–168, 2018.

[63] R. Majumder, “Some Aspects of Stability in Microgrids,” *IEEE Trans. Power Syst.*,

vol. 28, no. 3, pp. 3243–3252, 2013.

[64] A. Khodaei, “Provisional Microgrid Planning,” *IEEE Trans. Smart Grid*, vol. 8, no. 3, pp. 1096-1104, May 2017.

[65] W. Shi, X. Xie, C. Chu, and R. Gadh, “Distributed Optimal Energy Management in Microgrids,” *IEEE Trans. Smart Grid*, vol. 6, no. 3, pp. 1137–1146, 2015.

[66] F. Wu, X. Li, F. Feng, and H. B. Gooi, “Modified cascaded multilevel grid-connected inverter to enhance European efficiency and several extended topologies,” *IEEE Trans. Ind. Informatics*, vol. 11, no. 6, pp. 1358–1365, 2015.

[67] M. J. Sanjari, A. H. Yatim, and G. B. Gharehpetian, “Online dynamic security assessment of microgrids before intentional islanding occurrence,” *Neural Comput. Appl.*, vol. 26, no. 3, pp. 659–668, 2015.

[68] M. Shahidehpour and J. F. Clair, “A Functional Microgrid for Enhancing Reliability, Sustainability, and Energy Efficiency,” *Electr. J.*, vol. 25, no. 8, pp. 21–28, 2012.

[69] “Microgrid Deployment Tracker 4Q13; Commercial/Industrial, Community/Utility, Institutional/Campus, Military, and Remote Microgrids: Operating, Planned, and Proposed Projects by World Region,” 2013.

[70] “Microgrid Deployment Tracker 2Q16,” *Navigant Research*, 2016. [Online]. Available: https://www.navigantresearch.com/research/microgrid-deployment-tracker-2q16.

[71] A. Majzoobi, A. Khodaei, S. Bahramirad, and M. H. J. Bollen, “Capturing the variabilities of distribution network net-load via available flexibility of microgrids,” in *Grid of the Future Symposium (CIGRE)*, Philadelphia, PA, 2016.

[72] A. Majzoobi and A. Khodaei, "Application of Microgrids in Addressing Distribution Network Net-Load Ramping," *2016 IEEE PES Innovative Smart Grid Technologies (ISGT)*, Minneapolis, MN, Sept. 2016.

[73] A. Majzoobi and A. Khodaei, "Leveraging microgrids for capturing uncertain distribution network net load ramping," *NAPS 2016 - 48th North Am. Power Symp.,* Denver, CO, Sept. 2016.

[74] N. Holjevac, T. Capuder, and I. Kuzle, "Adaptive control for evaluation of flexibility benefits in microgrid systems," *Energy*, vol. 92, pp. 487–504, 2015.

[75] S. I. Vagropoulos and A. G. Bakirtzis, "Optimal Bidding Strategy for Electric Vehicle Aggregators in Electricity," vol. 28, no. 4, pp. 4031–4041, 2013.

[76] H. Kim and M. Thottan, "A two-stage market model for microgrid power transactions via aggregators," *Bell Labs Tech. J.*, vol. 16, no. 3, pp. 101–107, 2011.

[77] D. T. Nguyen and L. B. Le, "Risk-constrained profit maximization for microgrid aggregators with demand response," *IEEE Trans. Smart Grid*, vol. 6, no. 1, pp. 135–146, 2015.

[78] M. J. Sanjari, H. Karami, and H. B. Gooi, "Micro-generation dispatch in a smart residential multi-carrier energy system considering demand forecast error," *Energy Convers. Manag.*, vol. 120, pp. 90–99, 2016.

[79] L. Shi, Y. Luo, and G. Y. Tu, "Bidding strategy of microgrid with consideration of uncertainty for participating in power market," *Electr. Power Energy Syst.*, vol. 59, pp. 1–13, 2014.

[80] Y. Gu and L. Xie, "Stochastic Look-Ahead Economic Dispatch With Variable

Generation Resources," *IEEE Trans. Power Syst.*, pp. 1–13, 2016.

[81] A. Majzoobi and A. Khodaei, "Application of Microgrids in Supporting Distribution Grid Flexibility," *IEEE Trans. Power Syst.*, vol. 32, no. 1, pp. 17-29, Jan. 2017.

[82] "Estimating the Value of Lost Load." [Online]. Available: http://www.ercot.com/content/gridinfo/resource/2015/mktanalysis/ERCOT_ValueofLostLoad_LiteratureReviewandMacroeconomic.pdf.

[83] A. Khodaei, "Microgrid optimal scheduling with multi-period islanding constraints," *IEEE Trans. Power Syst.*, vol. 29, no. 3, pp. 1383–1392, 2014.

[84] A. Majzoobi and A. Khodaei, "Application of microgrids in providing ancillary services to the utility grid," *Energy*, vol. 123, pp. 555-563, Mar. 2017.

[85] A. Khodaei, S. Bahramirad, and M. Shahidehpour, "Microgrid Planning Under Uncertainty," *IEEE Trans. Power Syst.*, vol. 30, no. 5, pp. 2417–2425, 2015.

[86] A. Khodaei, "Resiliency-oriented microgrid optimal scheduling," *IEEE Trans. Smart Grid*, vol. 5, no. 4, pp. 1584–1591, 2014.

[87] A. Y. Saber and G. K. Venayagamoorthy, "Resource scheduling under uncertainty in a smart grid with renewables and plug-in vehicles," *IEEE Syst. J.*, vol. 6, no. 1, pp. 103–109, 2012.

[88] N. Nikmehr and S. Najafi-Ravadanegh, "Optimal operation of distributed generations in micro-grids under uncertainties in load and renewable power generation using heuristic algorithm," *IET Renew. Power Gener.*, vol. 9, no. 8, pp. 982–990, 2015.

[89] J. Wen, X. Han, J. Li, Y. Chen, H. Yi, and C. Lu, "Transmission network expansion

planning considering uncertainties in loads and renewable energy resources," *CSEE J. Power Energy Syst.*, vol. 1, no. 1, pp. 78–85, 2015.

[90] A. Majzoobi, A. Khodaei, and S. Bahramirad, "Capturing Distribution Grid-Integrated Solar Variability and Uncertainty Using Microgrids," *IEEE Power and Energy Society General Meeting*, Chicago, IL, July 2017, pp. 1–5.

[91] G. Ferruzzi, G. Cervone, L. Delle Monache, G. Graditi, and F. Jacobone, "Optimal bidding in a Day-Ahead energy market for Micro Grid under uncertainty in renewable energy production," *Energy*, vol. 106, pp. 194–202, 2016.

[92] H. Lotfi and A. Khodaei, "An efficient preprocessing approach for uncertainty consideration in microgrids," *2016 IEEE/PES Transmission and Distribution Conference and Exposition (T&D)*, Dallas, TX, 2016, pp. 1-5

[93] R. Eskandarpour and A. Khodaei, "Leveraging Accuracy-Uncertainty Tradeoff in SVM to Achieve Highly Accurate Outage Predictions," *IEEE Trans. Power Syst.*, vol. 33, no. 1, pp. 1139–1141, 2018.

[94] A. Khodaei and M. Shahidehpour, "Microgrid-based co-optimization of generation and transmission planning in power systems," *IEEE Trans. Power Syst.*, vol. 28, no. 2, pp. 1582–1590, 2013.

[95] "PeakLab." [Online]. Available: https://portfolio.du.edu/peaklab.

[96] "Microgrid Deployment Tracker 2Q18," *Navigant Research*. [Online]. Available: https://www.navigantresearch.com/reports/microgrid-deployment-tracker-2q18.

[97] "Microgrid Deployment Tracker 4Q18," *Navigant Research*. [Online]. Available: https://www.navigantresearch.com/reports/microgrid-deployment-tracker-4q18.

[98] A. Albaker, A. Majzoobi, G. Zhao, J. Zhang, and A. Khodaei, “Privacy-preserving optimal scheduling of integrated microgrids,” *Electr. Power Syst. Res.*, vol. 163, pp. 164–173, Oct. 2018.

[99] M. Lazzaro *et al.*, “Flexibility Services to Power Systems from Smart Rural Microgrid Prosumers,” *2018 IEEE International Conference on Environment and Electrical Engineering and 2018 IEEE Industrial and Commercial Power Systems Europe (EEEIC / I&CPS Europe)*, Palermo, 2018, pp. 1-6.

[100] S. Gottwalt, J. Gärttner, H. Schmeck, and C. Weinhardt, “Modeling and Valuation of Residential Demand Flexibility for Renewable Energy Integration,” *IEEE Trans. Smart Grid*, vol. 8, no. 6, pp. 2565–2574, 2017.

[101] Q. Dang and Y. Huo, “Flexibility Scheduling for Microgrids with Electric Vehicle (EV) Penetration,” in *2018 IEEE Energy Conversion Congress and Exposition (ECCE)*, 2018, pp. 1078–1083.

[102] L. Zhang *et al.*, “Multi-Objective Day-Ahead Optimal Scheduling of Isolated Microgrid Considering Flexibility,” *E3S Web Conf.*, vol. 53, 2018.

[103] S. Parhizi, A. Khodaei, and M. Shahidehpour, “Market-Based Versus Price-Based Microgrid Optimal Scheduling,” *IEEE Trans. Smart Grid*, vol. 9, no. 2, pp. 615–623, 2018.

[104] S. Parhizi, A. Majzoobi, and A. Khodaei, “Net-zero settlement in distribution markets,” in *IEEE Power and Energy Society General Meeting*, Chicago, IL, July 2017, pp. 1–5.

[105] A. Majzoobi, M. Mahoor, and A. Khodaei, “Distribution Market as a Ramping

Aggregator for Grid Flexibility Support," in *2018 IEEE/PES Transmission and Distribution Conference and Exposition (T&D)*, Denver, CO, Apr. 2018, pp. 1–9.

Appendix A: List of Publications

- **Journal Papers:**

1. M. Mahoor, **A. Majzoobi** and A. Khodaei, "Distribution Asset Management through coordinated microgrid scheduling," *IET Smart Grid,* vol. 1, no. 4, pp. 159-168, Dec. 2018.

2. A. Albaker, **A. Majzoobi**, G. Zhao, J. Zhang, A. Khodaei, "Privacy-Preserving Optimal scheduling of Integrated microgrids," *Electric power system research,* vol. 163 part (A), pp. 164-173, Oct. 2018.

3. **A. Majzoobi,** A. Khodaei, "Application of microgrids in providing ancillary services to the utility grid," *Energy,* vol. 123, pp. 555-563, Mar. 2017.

4. **A. Majzoobi,** A. Khodaei, "Application of microgrids in supporting distributed grid flexibility," *IEEE Transactions on Power Systems,* vol. 32, no. 5, pp. 3660-3669, Sept. 2017.

- **Conference Papers:**

1. A. Abiri-Jahromi, **A. Majzoobi**, A. Khodaei, S. Bahramirad, L. Zhang, A. Paaso, M. Lelic, D. Flinn, "Battery energy storage requirements for mitigating PV output fluctuations," 2018 IEEE PES Innovative Smart Grid Technologies Conference Europe (ISGT-Europe), Sarajevo, 2018, pp. 1-5.

2. **A. Majzoobi**, M. Mahoor, A. Khodaei, "Distribution market as a ramping aggregator for grid flexibly support," in IEEE PES Transmission and Distribution (T&D), Denver, CO, Apr. 2018.

3. M. Mahoor, **A. Majzoobi**, Z. S. Hosseini, A. Khodaei, "Leveraging sensory data in estimating transformer lifetime," in North American Power Symposium (NAPS), Morgantown, WV, Sept. 2017.

4. **A. Majzoobi**, M. Mahoor, A. Khodaei, "Machine learning applications in estimating transformer loss of life," in IEEE Power & Energy Society General Meeting, Chicago, IL, July 2017.

5. **A. Majzoobi**, A. Khodaei and S. Bahramirad, "Capturing distribution grid-integrated solar variability and uncertainty using microgrids," in IEEE Power & Energy Society General Meeting, Chicago, IL, July 2017.

6. S. Parhizi, **A. Majzoobi** and A. Khodaei, "Net-Zero settlement in distribution markets," IEEE Power & Energy Society General Meeting, Chicago, IL, July 2017.

7. **A. Majzoobi** and A. Khodaei, "Leveraging microgrids for capturing uncertain distribution network net load ramping," in North American Power Symposium (NAPS), Denver, CO, Sept. 2016.

8. **A. Majzoobi** and A. Khodaei, "Application of microgrids in addressing distribution network net-load ramping," in Innovative Smart Grid Technologies Conference (ISGT), Minneapolis, MN, Sept. 2016.

9. H. Lotfi, **A. Majzoobi**, A. Khodaei, S. Bahramirad, A. Paaso, "Levelized cost of energy calculation for energy storage systems," in CIGRE Grid of the future symposium, Philadelphia, PA, 2016.

10. **A. Majzoobi**, A. Khodaei, S. Bahramirad, M. Bollen, "Capturing the variabilities of distribution network net-load via available flexibility of microgrids," in CIGRE Grid of the future symposium, Philadelphia, PA, 2016.